Miao HQ, Lee P, Lin H, Soker S, Klagsbrun M. (2000). Neuropilin-1 expression by tumor cells promotes tumor angiogenesis and progression. *FASEB J* **14**: 2532–2539.

Parikh AA, Fan F, Liu WB, Ahmad SA, Stoeltzing O, Reinmuth N *et al.* (2004). Neuropilin-1 in human colon cancer: expression, regulation, and role in induction of angiogenesis. *Am J Pathol* **164**: 2139–2151.

Rieger J, Wick W, Weller M. (2003). Human malignant glioma cells express semaphorins and their receptors, neuropilins and plexins. *Glia* **42**: 379–389.

West DC, Rees CG, Duchesne L, Patey SJ, Terry CJ, Turnbull JE *et al.* (2005). Interactions of multiple heparin binding growth factors with neuropilin-1 and potentiation of the activity of fibroblast growth factor-2. *J Biol Chem* **280**: 13457–13464.

Wey JS, Gray MJ, Fan F, Belcheva A, McCarty MF, Stoeltzing O *et al.* (2005). Overexpression of neuropilin-1 promotes constitutive MAPK signalling and chemoresistance in pancreatic cancer cells. *Br J Cancer* **93**: 233–241.

Supplementary Information accompanies the paper on the Oncogene website (http://www.nature.com/onc).

# ELMO1 and Dock180, a Bipartite Rac1 Guanine Nucleotide Exchange Factor, Promote Human Glioma Cell Invasion

Michael J. Jarzynka,[1,2] Bo Hu,[1,3] Kwok-Min Hui,[1,2] Ifat Bar-Joseph,[1,2] Weisong Gu,[4] Takanori Hirose,[5] Lisa B. Haney,[7] Kodi S. Ravichandran,[7] Ryo Nishikawa,[6] and Shi-Yuan Cheng[1,2]

[1]Cancer Institute and Departments of [2]Pathology and [3]Medicine, University of Pittsburgh, Pittsburgh, Pennsylvania; [4]Ohio Supercomputer Center-Springfield, Springfield, Ohio; Departments of [5]Pathology and [6]Neurosurgery, Saitama Medical University, Moroyama-machi, Iruma-gun, Saitama, Japan; and [7]Beirne Carter Center for Immunology Research and Department of Microbiology, University of Virginia, Charlottesville, Virginia

## Abstract

**A distinct feature of malignant gliomas is the intrinsic ability of single tumor cells to disperse throughout the brain, contributing to the failure of existing therapies to alter the progression and recurrence of these deadly brain tumors. Regrettably, the mechanisms underlying the inherent invasiveness of glioma cells are poorly understood. Here, we report for the first time that engulfment and cell motility 1 (ELMO1) and dedicator of cytokinesis 1 (Dock180), a bipartite Rac1 guanine nucleotide exchange factor (GEF), are evidently linked to the invasive phenotype of glioma cells. Immunohistochemical analysis of primary human glioma specimens showed high expression levels of ELMO1 and Dock180 in actively invading tumor cells in the invasive areas, but not in the central regions of these tumors. Elevated expression of ELMO1 and Dock180 was also found in various human glioma cell lines compared with normal human astrocytes. Inhibition of endogenous ELMO1 and Dock180 expression significantly impeded glioma cell invasion *in vitro* and in brain tissue slices with a concomitant reduction in Rac1 activation. Conversely, exogenous expression of ELMO1 and Dock180 in glioma cells with low level endogenous expression increased their migratory and invasive capacity *in vitro* and in brain tissue. These data suggest that the bipartite GEF, ELMO1 and Dock180, play an important role in promoting cancer cell invasion and could be potential therapeutic targets for the treatment of diffuse malignant gliomas.** [Cancer Res 2007;67(15):7203–11]

## Introduction

The inherent invasive nature of malignant gliomas contributes to the high frequency of tumor recurrence and disease progression in patients afflicted with these deadly cancers. In spite of the use of multimodal therapies including surgery, radiation, and chemotherapy, the mean survival time in patients with high-grade gliomas is less than 1 year (1). It is established that the mechanisms regulating cell migration are fundamental to the invasive phenotype of gliomas (2). Although studies show that various stimuli promote glioma cell invasion, the mechanisms underlying dysregulation of cell motility during invasion of these tumor cells remain largely unknown.

Cell migration is highly regulated by spatial and temporal changes of the actin cytoskeleton essential for many physiologic and pathologic processes including cancer cell invasion. Rac1, a member of the Rho GTPase family, is a key regulator of actin cytoskeletal dynamics and relays signals from various stimuli such as growth factors, cytokines, and adhesion molecules to downstream effectors modulating cell migration and invasion (3). Importantly, Rac1 has been shown to promote glioma cell migration (4–10). The activation of Rac1 is through a GDP/GTP exchange mechanism catalyzed by the guanine nucleotide exchange factors (GEF) resulting in an active, GTP-bound state (11). The Rho GTPase GEFs are a large family of proteins that contain either a Dbl homology domain involved in nucleotide exchange (12) or a newly characterized Docker domain that facilitates GEF function (13), of which Dock180 (dedicator of cytokinesis 180) is the prototypical mammalian member.

Dock180 was first identified as a CrkII-binding protein that regulates NIH 3T3 cell morphology (14). Studies in *C. elegans* and *Drosophila* reveal that Dock180 homologues modulate various functions such as phagocytosis, cell migration, myoblast fusion, dorsal closure, and cytoskeletal organization through the activation of Rac1 (15–18). Furthermore, Dock180 stimulates phagocytosis and filopodia formation downstream of integrin receptor signaling in mammalian cells (19, 20). Importantly, Dock180 facilitates nucleotide exchange on Rac1 through its unconventional Docker GEF domain (21–23) but requires binding to engulfment and cell motility 1 (ELMO1) in achieving GDP/GTP exchange on Rac (21). In mammalian cells and in *C. elegans*, ELMO1 and its homologue, CED-12, enhance phagocytosis and cell migration by forming a complex with Dock180 (24). This bipartite GEF complex synergistically functions upstream of Rac1, promoting Rac-dependent cell migration (25). Although ELMO1 and Dock180 stimulate cell migration in normal mammalian cells, whether these molecules play a critical role in cancer cell migration and invasion has not been investigated.

In this study, we show for the first time that ELMO1 and Dock180 stimulate glioma cell migration and invasion. We detected high-level expression of ELMO1 and Dock180 in actively infiltrating glioma cells within the invasive regions along blood vessels, neuronal structures, and the corpus callosum as compared with the central tumor areas of primary human glioma specimens representing WHO grades 2 to 4. Furthermore, we found that ELMO1 and Dock180 expression is increased in human glioma cell lines compared with normal human astrocytes. Inhibition of

**Note:** Supplementary data for this article are available at Cancer Research Online (http://cancerres.aacrjournals.org/).

Current address for W. Gu: SuperArray Bioscience, 7320 Executive Park, Frederick, MD 21704.

**Requests for reprints:** Shi-Yuan Cheng, Cancer Institute and Department of Pathology, University of Pittsburgh, HCCLB, 2.26f, 5117 Centre Avenue, Pittsburgh, PA 15213. Phone: 412-623-3261; Fax: 412-623-4840; E-mail: chengs@upmc.edu or Bo Hu, Cancer Institute and Department of Medicine, University of Pittsburgh, HCCLB, 2.19f, 5117 Centre Avenue, Pittsburgh, PA 15213. Phone: 412-623-7791; Fax: 412-623-4840; E-mail: hub@upmc.edu.



doi:10.1158/0008-5472.CAN-07-0473

endogenous ELMO1 and Dock180 impeded glioma cell migration and invasion whereas forced expression of ELMO1 and Dock180 in glioma cell lines with low endogenous expression enhanced tumor cell migration and invasion *in vitro* and *ex vivo*. These data show a novel function for the bipartite GEF, ELMO1 and Dock180, in stimulating cancer cell migration and invasion.

## Materials and Methods

**Cell lines, antibodies, and reagents.** Human LN18, LN229, U118, and U87MG glioma cells were obtained from American Type Culture Collection; U251MG and U373MG glioma cells were from our collection and their culture was previously described (26). D54MG glioma cells were from Dr. D. Bigner (Duke University, Durham, NC). SNB19 glioma cells were from Dr. Y-H. Zhou (University of California, Irvine, Irvine, CA). Immortalized normal human astrocytes and genetically modified normal human astrocytes (27) were from Dr. R. Pieper (University of California, San Francisco, San Francisco, CA). The following reagents were used in our studies: goat anti-Dock180 antibody (H-4), goat anti-Dock180 antibody (N-19), and goat anti-β-actin (I-19) antibodies (Santa Cruz Biotechnology), goat anti-ELMO1 (Ab2239, Abcam), rabbit anti-ELMO1 antibody (21), Rac1 activation assay kit (Upstate Technology), and a mouse anti-Rac1 antibody (BD PharMingen). The secondary antibodies were from Vector Laboratories or Jackson ImmunoResearch Laboratories. A 3,3′-diaminobenzidine elite kit was from DAKO; AquaBlock was from East Coast Biologics, Inc. Cell culture media and other reagents were from Hyclone, Invitrogen BRL, Sigma Chemicals, and Fisher Scientific.

**Immunohistochemical analyses of primary human glioma specimens.** A total of 53 human malignant glioma specimens that contain an identifiable center and border/invasive area were used and included 6 diffuse astrocytomas (grade 2), 1 oligoastrocytoma (grade 2), 5 oligodendrogliomas (grade 2), 8 anaplastic astrocytomas (grade 3), 5 anaplastic oligodendrogliomas (grade 3), 3 anaplastic oligoastrocytomas (grade 3), and 25 glioblastoma multiforme (grade 4). Additionally, four normal human brain specimens obtained at autopsy from patients without brain lesions were included as controls. Immunohistochemical analyses and scoring were done as previously described (28) with no (−), weakest (±), low (1+), medium (2+), and strong (3+) staining with a polyclonal rabbit anti-ELMO1 (1:150) and a polyclonal goat anti-Dock180 (N-19; 1:1,000) antibody.

**Microdissection and protein extraction of paraffin-embedded glioma tissue.** Microdissection of paraffin-embedded human glioma tissue was done as previously described (28). Briefly, the paraffin-embedded glioma specimens were sectioned at 5- and 50-μm thicknesses and mounted onto glass slides. To identify the center, border, and invasive regions within the glioma specimen, the 5-μm-thick sections were stained with H&E. Three 50-μm-thick sister sections of each sample were then deparaffinized in xylenes, rehydrated in graded ethanol, immersed in distilled water, and air-dried. To exclusively collect the center or border regions of the tissue, the targeted areas were cut microscopically under an Olympus SZ-STS stereomicroscope with a fine needle using the sister H&E-stained section as a guide. Next, total protein was extracted from the microdissected, formalin-fixed paraffin-embedded glioma tissue as previously described (28).

**Immunoblotting.** Thirty micrograms of total protein from various whole-cell lysates were separated by NuPAGE 10% Bis-Tris polyacrylamide gel (Invitrogen) electrophoresis under reducing conditions and transferred onto Immobilon-P transfer membranes (Millipore). The membranes were blocked, incubated with the indicated primary antibodies, and subsequently probed with peroxidase-labeled secondary antibodies. The reacted proteins were visualized by enhanced chemiluminescence reaction (Amersham Biosciences).

**Inhibition of ELMO, Dock180, and Rac1 expression.** Small interfering RNA (siRNA) was synthesized by Invitrogen. The target sequences of ELMO1 were 5′-GGCACUAUCCUUCGAUUAACCACAU-3′ (designated E1) and 5′-CCGAGAGGAUGAACCAGGAAGAUUU-3′ (designated E2; ref. 29). The target sequences of Rac1 were 5′-AAGGAGAUUGGUGCUGUAAAA-3′ (designated R1; ref. 6) and 5′-AACCUUUGUACGCUUUGCUCA-3′ (designated R2; refs. 6, 7). A pool containing three separate Dock180 siRNAs was from Santa Cruz Biotechnology. The glioma cells were plated at 40% to 50% confluency, were allowed to attach to the tissue culture dish for ~3 h, and transfected with 60 to 120 nmol/L of the indicated siRNA for 24 h in the presence of 10% fetal bovine serum (FBS) in DMEM using Lipofectamine 2000 following the manufacturer's instructions (Invitrogen). Mock transfection was done in parallel using the Stealth RNAi Negative Control Med GC (Invitrogen). After 24 h, the siRNA/lipid complexes were removed and the cells were maintained in complete medium for an additional 48 h or treated with the proteasome inhibitors MG132 (2 μmol/L) or ALLN (4 μmol/L) for 24 h. The inhibition of protein expression was determined by Western blot analysis.

**Exogenous expression of ELMO1 and Dock180.** A pCG plasmid encoding c-Myc– and His-tagged full-length human ELMO1 (from Dr. J. Skowronski, Cold Spring Harbor Laboratory, Cold Spring Harbor, NY; ref. 30) and/or a pCXN2 plasmid encoding Flag-tagged full-length human Dock180 (from Dr. M. Matsuda, Kyoto University, Kyoto, Japan) was transfected into U87MG and U251MG cells using Effectene following the manufacturer's instructions (Qiagen). Forty-eight hours posttransfection, the cells were used in *in vitro* cell migration, invasion, and *ex vivo* brain slice assays. The expression of exogenous ELMO1 and Dock180 expression was determined by Western blot analysis.

**Rac1 activation assay.** GTP loading of Rac1 was measured using the Rac1 Activation Assay Kit (Upstate Technology) according to the manufacturer's instructions. Briefly, cells were lysed in ice-cold magnesium lysis buffer and cleared with glutathione-agarose beads. Cell extracts were then incubated with PAK-1 PBD agarose beads, pelleted, and washed. The beads were resuspended in sample buffer and separated by 10% PAGE. GTP-bound Rac1 was detected using an anti-Rac1 antibody.

***In vitro* migration and invasion assays.** *In vitro* migration and invasion assays were done as previously described (31). Briefly, 50 μL of transiently transfected (siRNA or plasmid DNA) glioma cells ($5 \times 10^5$/mL in serum-free DMEM plus 0.05% bovine serum albumin) were separately placed into the top compartment of a Boyden chamber. For migration assays, the cells were allowed to migrate through an 8-μm pore size membrane precoated with fibronectin (10 μg/mL) overnight at 37°C. For invasion assays, the cells were allowed to invade through a growth factor–reduced Matrigel–coated (0.78 mg/mL) membrane overnight at 37°C. Afterwards, the membrane was fixed and stained, nonmigrating and noninvading cells were removed, and the remaining cells were counted.

***Ex vivo* brain slice invasion assay.** The *ex vivo* brain slice assay was done as previously described with minor modifications (9, 10). Briefly, fresh sections (500-μm thickness) of mouse cerebrum from 8-week-old mice (C57/BL6, The Jackson Laboratory) were placed onto transwell membranes (0.4 μm pore size, Corning) in a six-well dish containing DMEM with 10% FBS, 100 units/mL of penicillin, and 100 μg/mL of streptomycin, allowing the surface of the brain slice to be semidry. Afterwards, green fluorescent protein (GFP)–expressing glioma cells ($5 \times 10^4$ in 0.5-μL DMEM) are placed onto the putamen of both sides of each brain slice and incubated in a humidified environment at 37°C, 5% $CO_2$ and 95% air. After 48 h, the brain slices were gently rinsed with PBS and fixed in 4% paraformaldehyde overnight at 4°C. Lateral cell migration/invasion was assessed by direct epifluorescent examination of GFP-expressing glioma cells using a stereomicroscope (SZX12, Olympus) at ×10 magnification. Images were captured with a SPOT digital camera (Diagnostic Instrument). Depth of cell invasion into the brain slice was determined by optical sectioning using a Zeiss LSM 510 Confocal Microscope (Carl Zeiss MicroImaging, Inc.).

**Statistical analysis.** One-way ANOVA with Newman-Keuls posttest or paired two-way Student's *t* test was done using GraphPad Prism version 4.00 for Windows (GraphPad software). A $\chi^2$ test was done as previously described to examine the association between immunohistochemical staining for ELMO1 and Dock180 and glioma invasion (28). $P < 0.05$ was considered statistically significant.

## Results

**ELMO1 and Dock180 are co-overexpressed in actively invading glioma cells of primary human glioma specimens.**

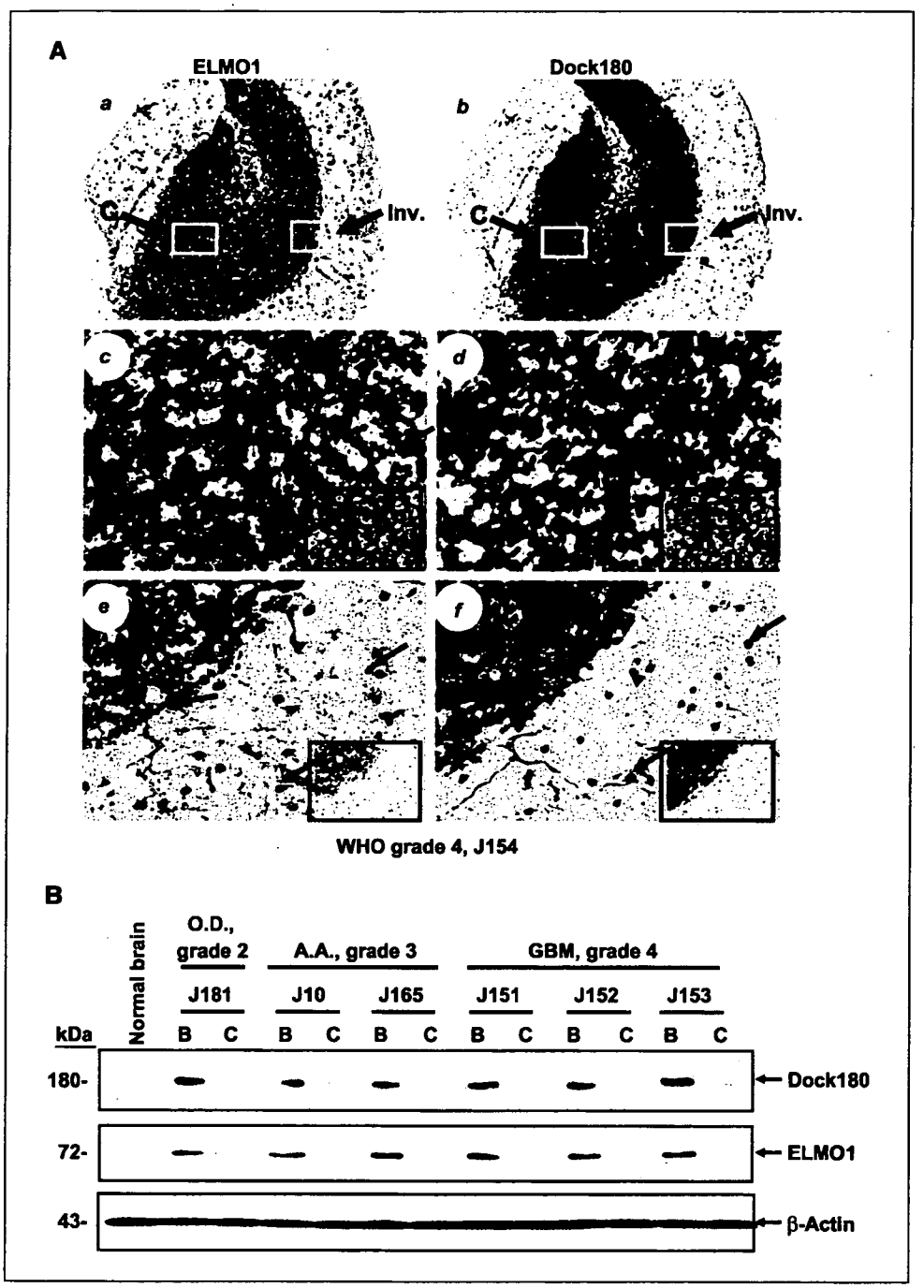


**Figure 1.** ELMO1 and Dock180 are co-overexpressed in invading tumor cells of primary human glioma specimens. *A*, a total of 53 individual primary tumor specimens (WHO grades 2–4) were analyzed, and representative staining of serial sections of glioblastoma multiforme (specimen J154, grade 4) tissue using a polyclonal rabbit anti-ELMO1 antibody (*a*, *c*, and *e*) and a polyclonal goat anti-Dock180 antibody (*b*, *d*, and *f*) is shown. *c* to *f*, *insets*, isotype-matched immunoglobulin G controls of the identical areas shown. *c* and *d*, enlarged central regions of the tumor mass shown in *a* and *b* (*white rectangle*). *e* and *f*, enlarged invasive areas shown in *a* and *b* (*red rectangle*). *Arrows*, positive staining for ELMO1 (*c* and *e*) and Dock180 (*f*). *Arrowheads*, unstained cells. Original magnification, ×100 (*a* and *b*); 400× (*c–f*). Representative results; immunohistochemical (*IHC*) analyses were done two additional times with similar results. *B*, immunoblot analysis of the tumor center (*C*) and invasive border (*B*) of primary glioma specimens. Total protein extracted from normal brain and microdissected glioma tissue from oligodendroglioma (*O.D.*; specimen J181, grade 2), anaplastic astrocytoma (*A.A.*; specimens J10 and J165, grade 3), and glioblastoma multiforme (*GBM*; specimens J151, J152, and J153, grade 4) was examined by immunoblotting with anti-Dock180 and anti-ELMO1 antibodies, respectively. The membranes were also probed with an anti–β-actin antibody as a loading control. Representative of three independent experiments with similar results.

The ELMO1-Dock180 complex has been shown to stimulate cell migration through the activation of Rac1 (25). Recently, we identified the up-regulation of ELMO1 gene expression in an angiopoietin-2–induced astrocytoma invasion model using global gene array followed by real-time PCR analysis,[8] signifying the potential importance of ELMO1 in promoting glioma invasion. To determine the role of ELMO1 and its binding partner Dock180 (21) in glioma cell invasion, we began by carrying out immunohistochemical analyses on a collection of primary human glioma specimens to assess whether ELMO1 and Dock180 are associated with the invasive phenotype of gliomas. We examined 53 tumors representing WHO grades 2 to 4 containing an identifiable central region and invasive areas and four normal human brain specimens (J140–J143) obtained at autopsy from patients without brain lesions as controls (28). Little to no immunoreactivity for ELMO1 and Dock180 was detected in the normal brain specimens (Supplementary Table S1; Fig. S1, *a* and *b*). Interestingly, the co-overexpression of ELMO1 and Dock180 was found in infiltrating tumor cells within the invasive areas of the glioma specimens independent of tumor grade (Fig. 1*A*, *e* and *f*; Supplementary

[8] Manuscript in preparation.

**Table 1.** ELMO1 and Dock180 expression correlates with glioma invasion

| Immunohistochemical score | ELMO1 | | | Dock180 | | |
|---|---|---|---|---|---|---|
| | Center | Border | Invasive | Center | Border | Invasive |
| 3+ | 0 | 3 | 9 | 0 | 3 | 10 |
| 2+ | 1 | 12 | 19 | 1 | 15 | 22 |
| 1+ | 9 | 14 | 7 | 3 | 15 | 15 |
| ± | 29 | 15 | 10 | 18 | 16 | 5 |
| − | 14 | 9 | 8 | 31 | 4 | 1 |
| *P* value of correlation between positivity and tumor area* | | | | | | |
| Border vs center | | <0.01 | | | <0.0001 | |
| Invasive vs center | | <0.0001 | | | <0.0001 | |
| Border vs invasive | | NS | | | <0.05 | |

NOTE: The immunohistochemical staining intensity for each antibody and specimen was defined as no (−), weakest (±), low (1+), medium (2+), and strong (3+) staining as previously described (28) and is shown in Supplementary Table S1. NS, not significant ($P > 0.05$).
*Analyzed by $\chi^2$ test for trend based on the distribution of the scores from each area.

Fig. S1, *e*, *f*, *i*, and *j*). Actively invading glioma cells observed at distant sites such as the gray matter of normal brain parenchyma, along blood vessels, neuronal structures, and the corpus callosum showed a high immunoreactivity for ELMO1 and Dock180 (data not shown). For example, in a glioblastoma multiforme (grade 4) specimen, the glioma cells invading into the adjacent brain structure (Fig. 1*A*, *e* and *f*, *arrows*) exhibited strong immunostaining by the ELMO1 and Dock180 antibodies. In contrast, Dock180 protein was not detected (Fig. 1*A*, *d*) and ELMO1 was expressed at low levels in the central core region of this same glioma tissue (Fig. 1*A*, *c*). Additionally, we failed to detect the expression of ELMO1 and Dock180 in reactive astrocytes or cells that are morphologically similar to astrocytes in invasive areas or center regions in these primary glioma specimens.

To determine whether there is a distinct link between ELMO1 and Dock180 expression and human glioma invasiveness, we did a $\chi^2$ test for trend to examine the association between the positive staining of ELMO1 and Dock180 and each area of the glioma specimen (center, border, and invasive areas). As shown in Table 1, a significant correlation was found between the positive immunoactivities for ELMO1 ($P < 0.01$ for border versus center and $P < 0.0001$ for invasive versus center, respectively) and Dock180 ($P < 0.0001$ for both comparisons) and the invasiveness displayed by these gliomas. Of the 53 glioma samples analyzed, 67% (8 of 12) and 92% (11 of 12) WHO grade 2 specimens, 69% (11 of 16) and 75% (12 of 16) grade 3 specimens, and 84% (21 of 25) and 96% (24 of 25) grade 4 specimens showed higher expression of ELMO1 and Dock180 in the border/invasive areas versus the center region of the tumors, respectively (Supplementary Table S1).

Next, to corroborate our observation of ELMO1 and Dock180 up-regulation in invading glioma cells of the primary glioma specimens, we did immunoblotting on total protein extracted from the border/invasive regions and core area of microdissected primary glioma tissues and four normal brain specimens (28) that were used in the immunohistochemical analyses. An increase in ELMO1 and Dock180 expression was found in the border region of all six primary glioma specimens examined when compared with the center tumor area of the identical sample (Fig. 1*B*). Little to no expression of ELMO1 and Dock180 was detected in the normal brain specimens (Fig. 1*B*; Supplementary Fig. S2). These findings

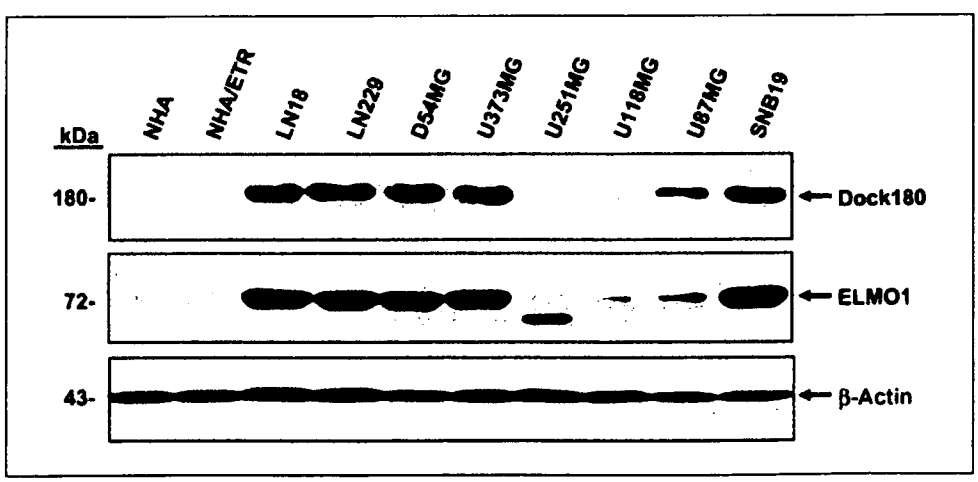


**Figure 2.** Endogenous expression of Dock180 and ELMO1 in various human glioma cell lines. Immunoblot analysis of normal human astrocytes (*NHA*), genetically modified normal human astrocytes (*NHA/ETR*; see Materials and Methods), and human glioma cell lysates with anti-Dock180 and anti-ELMO1 antibodies. The membranes were also probed with an anti–β-actin antibody as a loading control. Representative of three independent experiments with similar results.

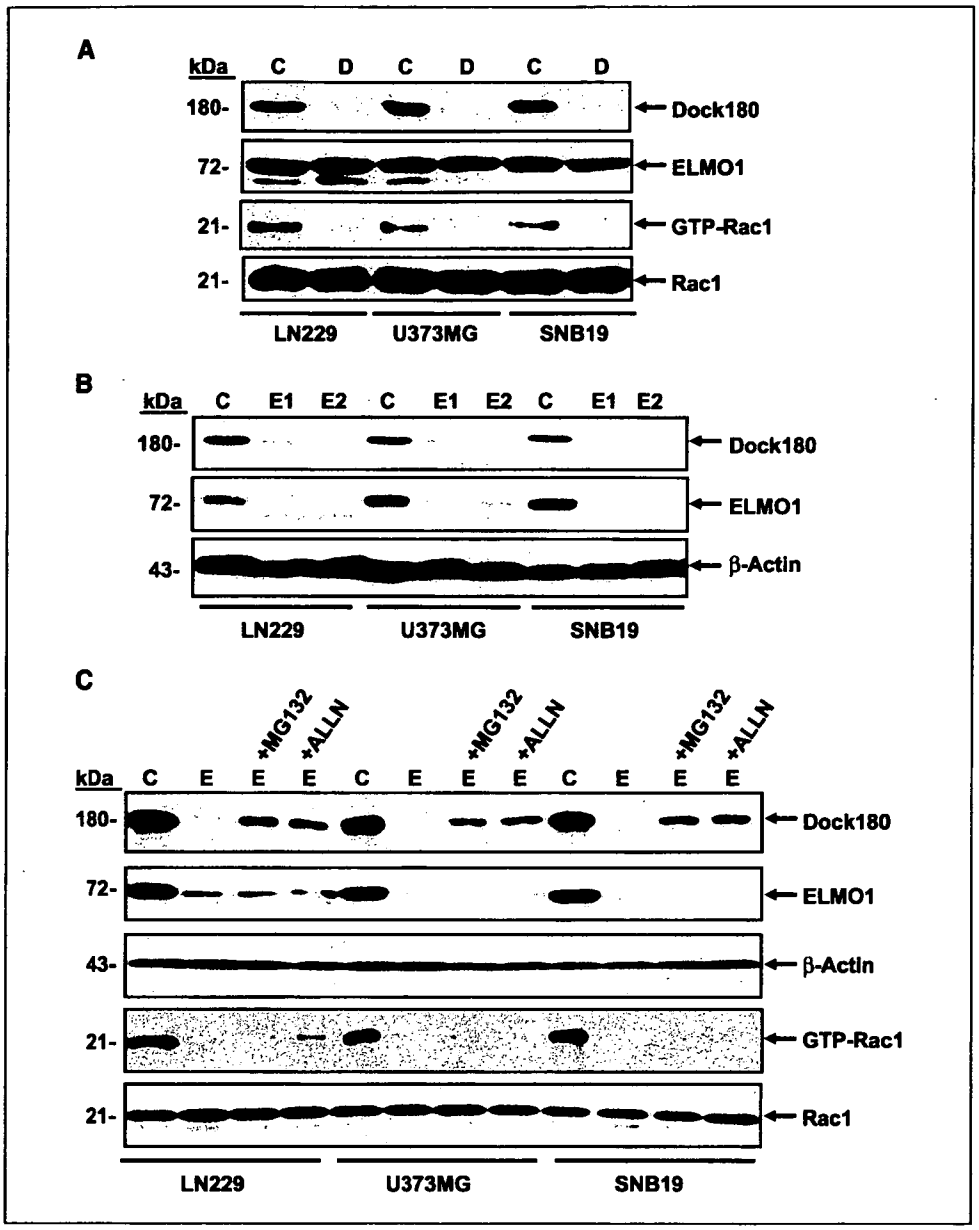


**Figure 3.** Suppression of endogenous ELMO1 and Dock180 inhibits GTP loading of Rac1 in glioma cells. *A* and *B*, LN229, U373MG, and SNB19 cells were transiently transfected with ELMO1 siRNA (*E1* and *E2*), Dock180 siRNA (*D*), or a control siRNA (*C*). Total cell lysates were analyzed by immunoblotting with anti-ELMO1, anti-Dock180, and anti-Rac1 antibodies and GTP loading of Rac1 using a Rac1 activation assay kit. *C*, LN229, U373MG, and SNB19 cells were transiently transfected with ELMO1 siRNA and treated with the proteasome inhibitors MG132 (2 μmol/L) or ALLN (4 μmol/L) followed by immunoblotting for ELMO1, Dock180, and Rac1 expression and GTP loading of Rac1. The membranes were also probed with an anti–β-actin antibody as a loading control. Representative of three independent experiments with similar results.

support our immunohistochemical data showing that ELMO1 and Dock180 are co-upregulated in the areas of active invasion of primary glioma specimens. Taken together, these data suggest that the expression of ELMO1 and Dock180 is consistent with the intrinsically invasive phenotype of gliomas and independent of tumor grade.

**ELMO1 and Dock180 are coexpressed in human glioma cell lines.** Next, we sought to determine whether ELMO1 and Dock180 play a role in glioma cell migration and invasion. We first examined the expression of ELMO1 and Dock180 in various human glioma cell lines. As shown in Fig. 2, LN18, LN229, D54MG, U373MG, and SNB19 glioma cell lines endogenously express ELMO1 and Dock180 at high levels whereas lower-level expression was found in normal human astrocytes, genetically modified normal human astrocytes (27), U251MG, U118, and U87MG glioma cell lines. In addition, the level of expression of ELMO1 correlated with the expression level of Dock180.

**Inhibition of endogenously expressed ELMO1 and Dock180 suppresses Rac1 activation in glioma cells.** ELMO1 and Dock180 have previously been shown to form a complex and act as a bipartite GEF thereby activating Rac1 (21). Therefore, we evaluated the significance of endogenous ELMO1 and Dock180 expression in glioma cells and determined whether inhibition of their expression by siRNA attenuates Rac1 activation. LN229, U373MG, and SNB19 glioma cells were separately transfected with ELMO1 and Dock180 siRNA. After 48 h, the glioma cells that were transiently transfected with a siRNA pool containing three target-specific sequences for Dock180 completely suppressed Dock180 expression and significantly attenuated Rac1 activation while having no effect on ELMO1 and Rac1 protein levels (Fig. 3*A*). Similarly, two different siRNAs for ELMO1 (designated E1 and E2) inhibited ELMO1 expression (Fig. 3*B*), resulting in a decrease in GTP loading of Rac1 without alteration of Rac1 protein expression (Fig. 3*C*). Interestingly, siRNA knockdown of ELMO1 also reduced the expression of Dock180 in

the glioma cells tested (Fig. 3*B* and *C*). This effect was partially blocked by the proteasome inhibitors MG132 and ALLN (Fig. 3*C*), corroborating a previous report showing that ELMO1 protects Dock180 from ubiquitylation-mediated degradation (29). These data suggest that ELMO1 and Dock180 function upstream of Rac1 and play an essential role in its activation in glioma cells.

**Suppression of endogenously expressed ELMO1 and Dock180 expression inhibits glioma cell migration and invasion.** Rac1, a Rho family GTPase member, induces lamellipodia formation, cell migration, and invasion in glioma cells (6). Therefore, we hypothesize that ELMO1 and Dock180 promote glioma cell migration and invasion through their effects on Rac1 activation. To test this hypothesis, we transiently transfected LN229, U373MG, and SNB19 glioma cells with ELMO1, Dock180, and Rac1 siRNA. As shown in Fig. 4*A* and Supplementary Fig. S3, suppression of ELMO1 and Dock180 expression inhibited *in vitro* glioma cell migration by 3- to 4-fold, comparable to Rac1 knockdown by siRNA (Supplementary Fig. S3). Consistent with these results, knockdown of endogenous ELMO1 and Dock180 inhibited the ability of LN229, U373MG, and SNB19 cells to invade through a growth factor–reduced Matrigel-coated membrane. Again, *in vitro* glioma cell invasion was attenuated to the same degree using ELMO1 or Dock180 siRNA as Rac1 suppression (Fig. 4*B*). These results suggest that ELMO1 and Dock180 have an essential role in promoting glioma cell migration and invasion similar to Rac1.

To test our hypothesis in a pathophysiologically relevant model, we examined whether inhibition of ELMO1 and Dock180 modulates the invasion of SNB19 and U373MG cells in a murine brain slice model (9, 10). We separately transfected GFP-expressing SNB19 and U373MG cells with control, ELMO1, or Dock180 siRNA. After 48 h, the glioma cells that were transfected with specific or control siRNAs were placed bilaterally onto the putamen of a murine brain slice and allowed to invade into the brain tissue for an additional 48 h. Afterwards, lateral migration/invasion and depth of invasion were evaluated. Inhibition of ELMO1 and Dock180 expression in both cell lines displayed less lateral migration/invasion on the brain slice compared with control siRNA–transfected or nontransfected cells (Fig. 4*C* and data not

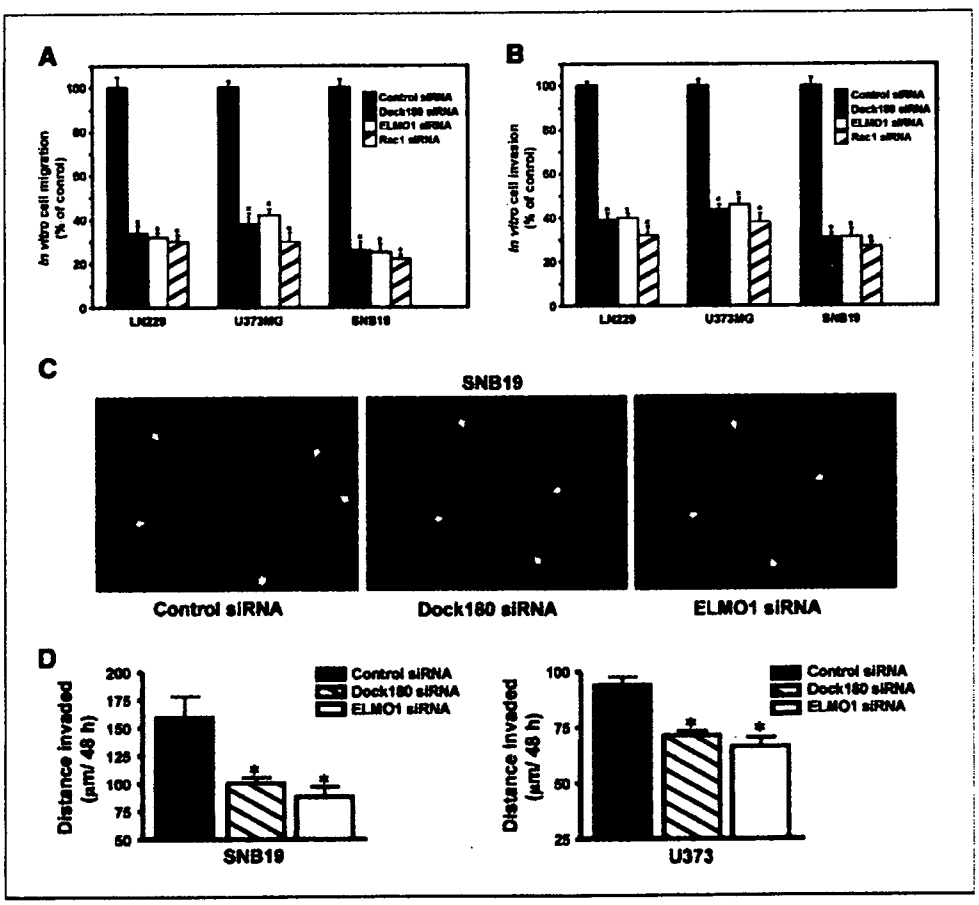


**Figure 4.** Suppression of endogenous ELMO1 and Dock180 inhibits glioma cell migration and invasion. *A, in vitro* cell migration assay. LN229, U373MG, and SNB19 cells were transiently transfected with the indicated siRNAs followed by cell migration assay. *B, in vitro* cell invasion assay. LN229, U373MG, and SNB19 cells were transiently transfected with the indicated siRNAs followed by an invasion assay. The migrating or invading cells were counted in 10 random high-powered fields (total magnification, ×200). Mean number of migrating or invading control cells: for migration, LN229 cells, 94.2 ± 4.6/field; U373MG cells, 73.1 ± 2.8/field; SNB19, 113.3 ± 3.8/field; and for invasion, LN229 cells, 46.7 ± 1.4/field; U373MG cells, 56.2 ± 1.9/field; SNB19, 37.2 ± 2.4/field. *Columns,* percent of control siRNA cells; *bars,* SD. *, $P < 0.05$, one-way ANOVA followed by Newman-Keuls post hoc. Three independent experiments were done in triplicate with similar results. *C,* GFP-expressing SNB19 and U373MG cells (data not shown) were transiently transfected with indicated siRNAs followed by an *ex vivo* brain slice invasion assay. Representative epifluorescent images of the GFP-expressing SNB19 cells were captured using a digital camera attached to a stereomicroscope at ×40 magnification. *D,* depth of SNB19 and U373MG cell invasion into a murine brain slice. *Columns,* mean distance (μm) invaded in 48 h from six independent experiments done in five to seven replicates per pair (control siRNA–transfected cells versus specific siRNA–transfected cells); *bars,* SE. *, $P < 0.05$, one-way ANOVA followed by Newman-Keuls post hoc. No-transfection controls for both SNB19 and U373MG cell lines were also done showing no observable effects on cell viability or the invasive ability when comparing the control siRNA–transfected and nontransfected cells (data not shown).

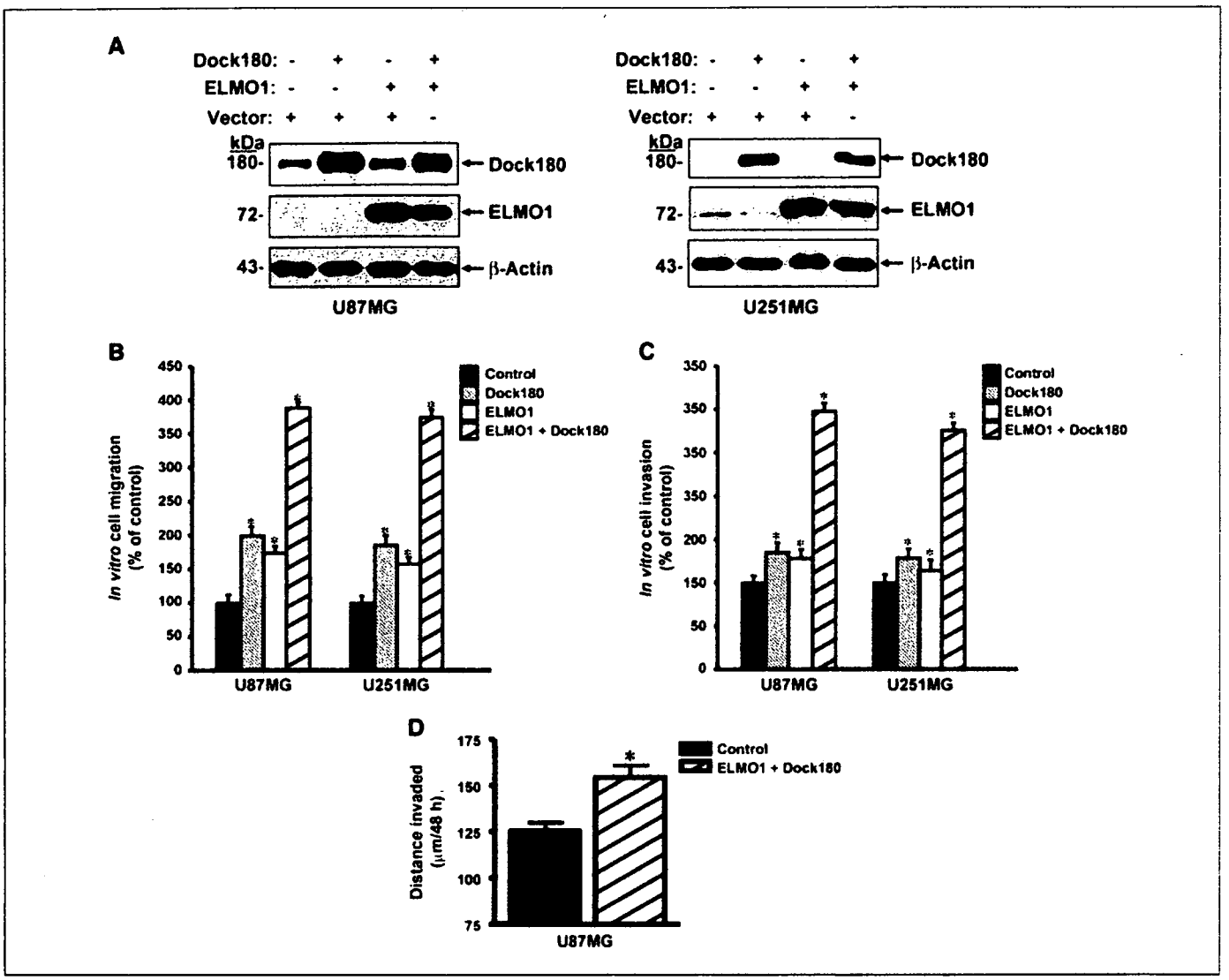


**Figure 5.** Exogenous expression of Dock180 and ELMO1 promotes glioma cell migration and invasion. *A*, U87MG and U251MG cells were transiently transfected with the indicated plasmids. Total cell lysates were analyzed by immunoblotting for ELMO1 and Dock180 expression. *B* and *C*, U87MG and U251MG cells were transiently transfected with the indicated plasmids followed by cell migration assay (*B*) or cell invasion assay (*C*). *D*, GFP-expressing U87MG cells were transiently transfected with the indicated plasmids and analyzed by an *ex vivo* brain slice invasion assay. *Columns*, mean distance (μm) invaded in 48 h from four independent experiments done in five to seven replicates per pair (control transfected–cells versus ELMO1- and Dock180-transfected cells); *bars*, SE. *, $P < 0.05$, paired Student's *t* test.

shown). Analysis by confocal laser scanning microscopy revealed that ELMO1 and Dock180 suppression significantly blocked the intrinsic invasiveness of the GFP-expressing SNB19 (mean ± SE, 88 ± 8.9 and 100 ± 5.2 μm/48 h, respectively) into the brain slice as compared with control siRNA–transfected or nontransfected SNB19 cells (mean ± SE, 159 ± 19 μm/48 h; Fig. 4*D* and data not shown). Similarly, glioma cell invasiveness was inhibited in the ELMO1 siRNA–treated (mean ± SE, 66 ± 4.1 μm/48 h) and Dock180 siRNA–treated (mean ± SE, 71 ± 2.2 μm/48 h) U373 cells versus the cells transfected with a control siRNA or nontransfected cells (mean ± SE, 94 ± 3.5 μm/48 h; Fig. 4*D* and data not shown). Thus, these results indicate that ELMO1 and Dock180 significantly contribute to the inherent invasive phenotype of these glioma cells *in vitro* and *ex vivo*.

**Exogenous expression of ELMO1 and Dock180 stimulates glioma cell migration and invasion.** In reciprocal experiments, we examined whether exogenous expression of ELMO1 and Dock180 in glioma cells that have low level endogenous expression increases glioma cell migration and invasion. First, U87MG and U251 glioma cells were transiently transfected with empty vectors, the ELMO1 and/or the Dock 180 plasmids leading to enhanced expression of these two proteins (Fig. 5*A*) and an increase in activated Rac1 (data not shown). Exogenous expression of ELMO1 and/or Dock180 in U87MG and U251MG cells increased cell migration and invasion *in vitro* with dual expression having the greatest effect of 3- to 4-fold (Fig. 5*B* and *C*).

Next, we tested whether exogenous overexpression of ELMO1 and Dock180 stimulates U87MG glioma cell invasion in the murine brain tissue. U87MG control (vector-transfected) and ELMO1/Dock180–expressing cells were separately seeded onto the murine brain slice. As shown in Fig. 5*D*, the depth of invasion into the brain slice was significantly increased in the ELMO1/Dock180–expressing

U87MG glioma cells (mean ± SE, 154 ± 6.5 μm/48 h) compared with the control transfected cells (mean ± SE, 125 ± 4.5 μm/48 h). Interestingly, the ELMO1/Dock180–expressing U87MG cells showed a similar invasion distance (mean ± SE, 154 ± 6.5 μm/48 h) as the parental SNB19 cells (mean ± SE, 159 ± 19 μm/48 h) that have high endogenous expression of ELMO1 and Dock180. Taken together, these results further confirm that ELMO1 and Dock180 are able to enhance the migration/invasion of glioma cells.

## Discussion

In the present study, we provide direct functional evidence showing that ELMO1 and Dock180 play a critical role in glioma invasion. Our data suggest that preferential expression of ELMO1 and Dock180 in invading glioma cells is associated with the intrinsically invasive behavior of human gliomas. Recent studies show that localized alterations in gene and protein expression in the actively invading glioma cell population may be responsible for their more migratory and invasive phenotype compared with the glioma cells of the tumor core (5, 9, 28, 32). Our results identify a significant correlation between ELMO1 and Dock180 expression and the invasive phenotype of the gliomas, strongly corroborating this theory. Immunohistochemical analysis revealed a co-overexpression of ELMO1 and Dock180 in the infiltrating glioma cells within the border and invasive regions compared with the central core of the identical glioma specimens, independent of WHO tumor grade. We witnessed glioma cells that were strongly positive for ELMO1 and Dock180 infiltrating along blood vessels, neuronal structures, and the corpus callosum (data not shown). This display of dissemination is consistent with the unique pattern of invasion of diverse anatomic structures observed in glioma biology (2). Importantly, because all malignant gliomas have the propensity to diffusely invade normal brain areas regardless of WHO grade (33), the increased expression of ELMO1 and Dock180 in the infiltrating tumor cells may reveal an important pathologic occurrence during active glioma cell invasion.

Dock180 and ELMO1 are evolutionarily conserved proteins that are essential in multiple biological processes involving cell migration (18, 24). For example, *myoblast city*, the Dock180 homologue in *Drosophila*, is necessary for dorsal closure and cytoskeletal organization in the migrating epidermis (16). CED-5 and CED-12, the homologues of Dock180 and ELMO1, are required for phagocytosis and cell migration in *C. elegans* (18, 24). In normal mammalian cells, ELMO1 and Dock180 form a complex, function as an unconventional Rac1-GEF (21), and stimulate cell migration through Rac1 activation (25). Notably, these latter studies use forced overexpression of ELMO1 and Dock180 in human embryonic kidney 293T and murine fibroblast LR73 cells to examine the effects of both proteins. In this study, we extended these observations for the first time to human glioma models revealing a novel function of this unconventional Rac1-GEF in promoting cancer cell migration and invasion. We found that inhibition of endogenously expressed ELMO1 and Dock180 attenuates the invasive behavior of glioma cell lines concomitant with a reduction in activated Rac1. Conversely, exogenous expression of ELMO1 and Dock180 in low-level expressing glioma cells increased their capacity to migrate and invade *in vitro* and in the brain, emphasizing the importance of these molecules in the invasive process of these malignant cells.

Tumor cell invasion requires both intrinsic cellular alterations and extrinsic stimuli to trigger cell motility (34). Our study examined how endogenously or exogenously expressed ELMO1 and Dock180 affected the intrinsic aspect of glioma cell migration and invasion independent of exogenous stimuli. The modest increase in invasion of ELMO1- and Dock180-overexpressing U87MG cells into the murine brain slice suggests the need for both intrinsic and extrinsic cues for efficient glioma invasion to occur. Indeed, the lack of exogenous stimuli and the diverse genetic background of glioma cell lines that impart distinct innate characteristics may influence the varying effects of ELMO1 and Dock180 on the invasive behavior of glioma cells. Because various growth factors such as epidermal growth factor (EGF), hepatocyte growth factor/scatter factor (HGF/SF), and platelet-derived growth factor (PDGF) have been implicated in promoting glioma cell invasion (35, 36), we investigated whether these growth factors regulate ELMO1 and Dock180. EGF, HGF/SF, and PDGF did not modulate the protein expression and phosphorylation of ELMO1 and Dock180 in glioma cells. Recent studies have shown that an EGF receptor (EGFR) mutant that lacks exons 3 to 7 of its extracellular domain (EGFRvIII) and is frequently found in high grade gliomas (1) promotes glioma progression and invasion in the brain (37, 38). We have found by immunohistochemical analysis that EGFRvIII is coexpressed with ELMO1 and Dock180 in invading tumor cells within the border regions but not in the center areas of primary glioma specimens. We are currently investigating the mechanisms by which ELMO1 and Dock180 mediate EGFRvIII-promoted glioma cell invasion using *in vitro* and *in vivo* models.

Rac1 regulates spatial and temporal changes of the actin cytoskeleton by relaying signals from various stimuli such as growth factors, cytokines, and adhesion molecules to downstream effectors (3) promoting glioma cell migration (4–10). Several reports indicate that activation of Rac1 by ephrin-B3 (9), fibroblast growth factor-inducible 14 (5), neurotensin (4), and P311 (39) stimulates glioma cell motility and invasion through actin cytoskeleton reorganization. It is plausible that ELMO1/Dock180 or other Rac1-GEFs (40) are responsible for mediating these upstream signals to activate Rac1 in these glioma cell lines, and thus further investigation is warranted.

It is well established that the tumor microenvironment composed of extracellular matrix contributes to the invasive behavior of gliomas (41–43). Cell adhesion to the extracellular matrix accomplished by cell-surface receptors such as integrins is a critical first step during glioma invasion (41). Dock180 has been shown to function downstream of the $\alpha_v\beta_5$ and $\beta_1$ integrins in GD25 fibroblasts and 293T cells, respectively (19, 20). Furthermore, a ternary complex consisting of RhoG-ELMO1-Dock180 mediates integrin-induced cell spreading of HeLa cells (44). Thus, integrin signaling may constitute another important pathway in facilitating ELMO1- and Dock180-mediated glioma invasion. Within the tumor microenvironment, the stromal cells serve as an ideal source of exogenous stimuli for glioma cells by producing numerous cytokines, proteases, and other extrinsic factors that affect cancer cell motility (34). Given that ELMO1 and Dock180 are co-overexpressed in actively infiltrating glioma cells, it is also possible that these extrinsic factors within the tumor milieu modulate ELMO1 and Dock180 expression through paracrine mechanisms.

In summary, this study identifies the novel function of the unconventional GEF, ELMO1 and Dock180, in promoting glioma cell migration and invasion. Co-overexpression of ELMO1 and Dock180 in actively infiltrating glioma cells illustrates a significant association between these Rac1 regulatory proteins and the invasive phenotype of diffuse gliomas. Because aberrant activation

of cell motility pathways may underlie cancer cell invasion, understanding the mechanisms by which ELMO1 and Dock180 mediate glioma cell invasion could establish these proteins as potential targets for effective therapies in the treatment of these deadly tumors.

## Acknowledgments

Received 2/5/2007; revised 4/8/2007; accepted 5/21/2007.

**Grant support:** NIH grant CA102011, American Cancer Society grant RSG CSM-107144 (S.Y. Cheng), and the Hillman Fellows Program (S-Y. Cheng and B. Hu).

The costs of publication of this article were defrayed in part by the payment of page charges. This article must therefore be hereby marked *advertisement* in accordance with 18 U.S.C. Section 1734 solely to indicate this fact.

We thank G. Wang for assistance in the use of laser confocal microscope, M. Nakada for help with the *ex vivo* brain slice invasion assay, J. Skowronski for the human ELMO1 plasmid and M. Matsuda for the human Dock180 plasmid, D. Bigner for the D54MG cells, Y-H. Zhou for the SNB19 cells, and R. Pieper for the immortalized normal human astrocytes and genetically modified normal human astrocytes.

## References

1. Maher EA, Furnari FB, Bachoo RM, et al. Malignant glioma: genetics and biology of a grave matter. Genes Dev 2001;15:1311–33.
2. Giese A, Bjerkvig R, Berens ME, Westphal M. Cost of migration: invasion of malignant gliomas and implications for treatment. J Clin Oncol 2003;21:1624–36.
3. Etienne-Manneville S, Hall A. Rho GTPases in cell biology. Nature 2002;420:629–35.
4. Servotte S, Camby I, Debeir O, et al. The in vitro influences of neurotensin on the motility characteristics of human U373 glioblastoma cells. Neuropathol Appl Neurobiol 2006;32:575–84.
5. Tran NL, McDonough WS, Savitch BA, et al. Increased fibroblast growth factor-inducible 14 expression levels promote glioma cell invasion via Rac1 and nuclear factor-κB and correlate with poor patient outcome. Cancer Res 2006;66:9535–42.
6. Chan AY, Coniglio SJ, Chuang YY, et al. Roles of the Rac1 and Rac3 GTPases in human tumor cell invasion. Oncogene 2005;24:7821–9.
7. Salhia B, Rutten F, Nakada M, et al. Inhibition of Rho-kinase affects astrocytoma morphology, motility, and invasion through activation of Rac1. Cancer Res 2005;65:8792–800.
8. Murai T, Miyazaki Y, Nishinakamura H, et al. Engagement of CD44 promotes Rac activation and CD44 cleavage during tumor cell migration. J Biol Chem 2004;279:4541–50.
9. Nakada M, Drake KL, Nakada S, Niska JA, Berens ME. Ephrin-B3 ligand promotes glioma invasion through activation of Rac1. Cancer Res 2006;66:8492–500.
10. Valster A, Tran NL, Nakada M, et al. Cell migration and invasion assays. Methods 2005;37:208–15.
11. Raftopoulou M, Hall A. Cell migration: Rho GTPases lead the way. Dev Biol 2004;265:23–32.
12. Hall A. Rho GTPases and the control of cell behaviour. Biochem Soc Trans 2005;33:891–5.
13. Meller N, Merlot S, Guda C. CZH proteins: a new family of Rho-GEFs. J Cell Sci 2005;118:4937–46.
14. Hasegawa H, Kiyokawa E, Tanaka S, et al. DOCK180, a major CRK-binding protein, alters cell morphology upon translocation to the cell membrane. Mol Cell Biol 1996;16:1770–6.
15. Kiyokawa E, Hashimoto Y, Kobayashi S, et al. Activation of Rac1 by a Crk SH3-binding protein, DOCK180. Genes Dev 1998;12:3331–6.
16. Erickson MR, Galletta BJ, Abmayr SM. *Drosophila* myoblast city encodes a conserved protein that is essential for myoblast fusion, dorsal closure, and cytoskeletal organization. J Cell Biol 1997;138:589–603.
17. Nolan KM, Barrett K, Lu Y, et al. Myoblast city, the *Drosophila* homolog of DOCK180/CED-5, is required in a Rac signaling pathway utilized for multiple developmental processes. Genes Dev 1998;12:3337–42.
18. Wu YC, Horvitz HR. *C. elegans* phagocytosis and cell-migration protein CED-5 is similar to human DOCK180. Nature 1998;392:501–4.
19. Albert ML, Kim JI, Birge RB. αvβ5 integrin recruits the CrkII-Dock180-1 complex for phagocytosis of apoptotic cells. Nat Cell Biol 2000;2:899–905.
20. Gustavsson A, Yuan M, Fallman M. Temporal dissection of β1-integrin signaling indicates a role for p130Cas-Crk in filopodia formation. J Biol Chem 2004;279:22893–901.
21. Brugnera E, Haney L, Grimsley C, et al. Unconventional Rac-GEF activity is mediated through the Dock180-ELMO complex. Nat Cell Biol 2002;4:574–82.
22. Cote JF, Vuori K. Identification of an evolutionarily conserved superfamily of DOCK180-related proteins with guanine nucleotide exchange activity. J Cell Sci 2002;115:4901–13.
23. Cote JF, Vuori K. *In vitro* guanine nucleotide exchange activity of DHR-2/DOCKER/CZH2 domains. Methods Enzymol 2006;406:41–57.
24. Gumienny TL, Brugnera E, Tosello-Trampont AC, et al. CED-12/ELMO, a novel member of the CrkII/Dock180/Rac pathway, is required for phagocytosis and cell migration. Cell 2001;107:27–41.
25. Grimsley CM, Kinchen JM, Tosello-Trampont AC, et al. Dock180 and ELMO1 proteins cooperate to promote evolutionarily conserved Rac-dependent cell migration. J Biol Chem 2004;279:6087–97.
26. Furnari FB, Lin H, Huang HS, Cavenee WK. Growth suppression of glioma cells by PTEN requires a functional phosphatase catalytic domain. Proc Natl Acad Sci U S A 1997;94:12479–84.
27. Sonoda Y, Ozawa T, Hirose Y, et al. Formation of intracranial tumors by genetically modified human astrocytes defines four pathways critical in the development of human anaplastic astrocytoma. Cancer Res 2001;61:4956–60.
28. Guo P, Imanishi Y, Cackowski FC, et al. Up-regulation of angiopoietin-2, matrix metalloprotease-2, membrane type 1 metalloprotease, and laminin 5γ2 correlates with the invasiveness of human glioma. Am J Pathol 2005;166:877–90.
29. Makino Y, Tsuda M, Ichihara S, et al. Elmo1 inhibits ubiquitylation of Dock180. J Cell Sci 2006;119:923–32.
30. Janardhan A, Swigut T, Hill B, Myers MP, Skowronski J. HIV-1 Nef binds the DOCK2-1 complex to activate rac and inhibit lymphocyte chemotaxis. PLoS Biol 2004;2:E6.
31. Hu B, Guo P, Fang Q, et al. Angiopoietin-2 induces human glioma invasion through the activation of matrix metalloprotease-2. Proc Natl Acad Sci U S A 2003;100:8904–9.
32. Demuth T, Berens ME. Molecular mechanisms of glioma cell migration and invasion. J Neurooncol 2004;70:217–28.
33. Kleihues P, Cavenee WK; International Agency for Research on Cancer. Pathology and genetics of tumours of the nervous system. Lyon: IARC Press; 2000. p. 314.
34. Sahai E. Mechanisms of cancer cell invasion. Curr Opin Genet Dev 2005;15:87–96.
35. Christofori G. New signals from the invasive front. Nature 2006;441:444–50.
36. Hamel W, Westphal M. Growth factors in gliomas revisited. Acta Neurochir (Wien) 2000;142:113–37; discussion 37–8.
37. Bachoo RM, Maher EA, Ligon KL, et al. Epidermal growth factor receptor and Ink4a/Arf: convergent mechanisms governing terminal differentiation and transformation along the neural stem cell to astrocyte axis. Cancer Cell 2002;1:269–77.
38. Wei Q, Clarke L, Scheidenhelm DK, et al. High-grade glioma formation results from postnatal Pten loss or mutant epidermal growth factor receptor expression in a transgenic mouse glioma model. Cancer Res 2006;66:7429–37.
39. McDonough WS, Tran NL, Berens ME. Regulation of glioma cell migration by serine-phosphorylated P311. Neoplasia 2005;7:862–72.
40. Rossman KL, Der CJ, Sondek J. GEF means go: turning on RHO GTPases with guanine nucleotide-exchange factors. Nat Rev Mol Cell Biol 2005;6:167–80.
41. Bellail AC, Hunter SB, Brat DJ, Tan C, Van Meir EG. Microregional extracellular matrix heterogeneity in brain modulates glioma cell invasion. Int J Biochem Cell Biol 2004;36:1046–69.
42. Giese A, Rief M, Loo M, Berens M. Determinants of human astrocytoma migration. Cancer Res 1994;54:3897–904.
43. Rao JS. Molecular mechanisms of glioma invasiveness: the role of proteases. Nat Rev Cancer 2003;3:489–501.
44. Katoh H, Negishi M. RhoG activates Rac1 by direct interaction with the Dock180-binding protein Elmo. Nature 2003;424:461–4.

Int J Clin Oncol (2007) 12:341–349
DOI 10.1007/s10147-007-0687-5



ORIGINAL ARTICLE

**Tomokazu Aoki · Ryo Nishikawa · Tomohiko Mizutani**
**Kuniharu Nojima · Kazuhiko Mishima · Jyunichi Adachi**
**Masao Matsutani**

# Pharmacokinetic study of temozolomide on a daily-for-5-days schedule in Japanese patients with relapsed malignant gliomas: first study in Asians

Received: January 15, 2007 / Accepted: May 1, 2007

**Abstract**
***Background.*** Temozolomide (TMZ) is widely used in Europe and the United States. For the safe use of TMZ in the Japanese, as representative of Asians, the pharmacokinetics of TMZ was investigated in Japanese patients and compared to that in Caucasians.
***Methods.*** The pharmacokinetics and safety of TMZ following oral administration of 150 and 200 mg/m$^2$ per day for the first 5 days of a 28-day treatment cycle were investigated in six Japanese patients with relapsed gliomas.
***Results.*** The time-to-maximum plasma concentration (tmax) of TMZ was about 1 h and the elimination half-life of terminal excretion phase ($t_{1/2}\lambda z$) was about 2 h. A dose-dependent increase was observed in maximum plasma concentration (Cmax) and AUC, while values for $t_{1/2}\lambda z$, apparent total body clearance (CL/F), and apparent distribution volume (Vz/F) were independent of dose. After administration for 5 days, changes in pharmacokinetics and accumulation were not observed. The plasma 5-(3-methyl)1-triazen-1-yl-imidazole-4-carboxamide (MTIC) concentration changed in parallel with the TMZ plasma concentration, and the Cmax and AUC of MTIC were about 2% of those of TMZ. The pharmacokinetic parameters of TMZ and MTIC in Japanese patients in this study were comparable to those previously determined in Caucasian subjects. Adverse events occurred in all patients, but toxicities were mostly mild or moderate, and continuation of administration was possible by adjusting the dose and by delaying the start of the next treatment cycle.
***Conclusion.*** The pharmacokinetic and safety profile of TMZ in Japanese patients was comparable to that in Caucasians. The treatment regimen used in Europe and the United States will be suitable for Asian patients, including Japanese.

**Key words** Malignant gliomas · Temozolomide · Pharmacokinetics · Japanese

T. Aoki (✉) · T. Mizutani · K. Nojima
Department of Neurosurgery, Kitano Hospital Medical Research Institute, 2-4-2 Ogimachi, Kita-ku, Osaka 530-8480, Japan
Tel. +81-6-6312-122; Fax +81-6-6361-0588
e-mail: tomokazu@kitano-hp.or.jp

R. Nishikawa · K. Mishima · J. Adachi · M. Matsutani
Department of Neurosurgery, Saitama Medical University, Saitama, Japan

## Introduction

The treatment of patients with malignant glioma remains the biggest challenge for the neuro-oncologist. Despite maximal safe surgical debulking and radiotherapy, overall survival for the average patient remains poor. In 1999, temozolomide (TMZ) was approved in the United States for refractory anaplastic astrocytoma and in the European Union for recurrent or progressed malignant glioma. In 2005, TMZ was additionally approved in the United States and the European Union for newly diagnosed glioblastoma multiforme, in combination with radiotherapy followed by monotherapy.

TMZ is an oral anticancer drug classified as an alkylating agent. In plasma, under physiological conditions, TMZ undergoes hydrolysis by rapid reaction with an alkaline base, and is transformed into 5-[(1Z)-3-methyltriaz-1-en-1-yl]-1H-imidazole-4-carboxamide (MTIC).[1–5] MTIC rapidly undergoes degeneration to the active form, methyldiazonium ion (DNA alkylating molecule)[3,5] and the inactive compound 5-aminoimidazole-4 carboxamide (AIC). TMZ has relatively high permeability through the blood-brain barrier as an unchanged drug.[6] These features contribute to its efficacy in patients with malignant gliomas.

Biological factors, including individual and ethnic differences, are considered to have little effect on the pharmacokinetics of TMZ. This consideration is based on the following findings: the bioavailability of TMZ with oral administration is nearly 100%,[7] linearity in pharmacokinetics is observed over a wide dose range,[8,9] the bioavailability of TMZ is not substantially affected by physiological conditions such as meals and gastric pH,[8,10] and the biotransformation from TMZ to MTIC and the formation of

methyldiazonium ion from MTIC are both nonenzymatic decomposition reactions.[1-5] Although TMZ is already being used in Taiwan and South Korea, no results have been reported of a pharmacokinetic study of TMZ in Asians.

We therefore investigated the pharmacokinetics of TMZ in Japanese patients, as representing Asians, to confirm its safety in Asian patients.

## Patients and methods

### Patient eligibility

Male and female patients with histologically proven relapsed gliomas with evidence of recurrence confirmed by magnetic resonance imaging (MRI) and whose Karnofsky performance status (KPS) was 50 or more were eligible for participation in this study. All pathology slides were reviewed by an independent central neuropathologist (Professor Yoichi Nakazato, Department of Human Pathology, Gunma University Graduate School of Medicine) based on WHO classification.[11] Patients also had to be 18 to less than 75 years in age, with male patients weighing at least 50 kg and female patients weighing at least 45 kg.

As prior treatment, patients must have undergone radiotherapy and chemotherapy. If the tumor was surgically resected at the time of relapse, MRI should have been conducted within 72 h after surgery and at least 8 days must have elapsed between the day of the surgery and the start of TMZ administration in the first cycle.

Patients also had to have an assessable tumor site confirmed by MRI, and the results of hematology and biochemistry tests had to meet defined criteria. Clinical laboratory values (performed within 14 days prior to TMZ [Temozolomide; Schering-Plough, Tokyo, Japan] administration, including the day of initial administration) had to be as follows: neutrophil count, $\geq 1500/mm^3$; platelet count, $\geq 100000/mm^3$; hemoglobin, ≥10.0 g/dl; blood urea nitrogen, <1.5 times the upper limit of laboratory standard value; serum creatinine, <1.5 times the upper limit of laboratory standard value; serum total bilirubin, ≤upper limit of laboratory standard value; transaminase, <3 times the upper limit of laboratory standard value; alkaline phosphatase, <2 times the upper limit of laboratory standard value.

Patients also had to have a life expectancy of at least 12 weeks.

This study was conducted after obtaining approval from the institutional review board at each study site. Written informed consent, according to the principles of the Declaration of Helsinki and the rules of Good Clinical Practice was obtained from all patients.

### Clinical endpoints

*Pharmacokinetics*

To examine the pharmacokinetics of TMZ in Japanese patients, pharmacokinetic parameters were calculated based on TMZ plasma concentrations, MTIC plasma concentrations, and TMZ urinary concentrations. The pharmacokinetic parameters of TMZ and MTIC plasma concentrations were then compared with those obtained in Caucasian patients.

*Safety*

Laboratory values (hematology, blood biochemistry, and urinalysis), body weight, body temperature, blood pressure, and pulse rate were measured, and adverse events and adverse reactions were investigated, according to the National Cancer Institute (NCI) common toxicity criteria (Version 2.0). The appropriateness of the safety evaluation made by the investigator was evaluated by an Efficacy and Safety Evaluation Committee (Yukitaka Ushio, Director of Otemae Hospital; Kazuo Tabuchi, Director of Koyanagi Memorial Hospital; and Professor Yuta Shibamoto, Department of Quantum Radiotherapy, Nagoya City University Graduate School of Medical Sciences).

### Treatment

One treatment cycle consisted of once-daily oral administration of TMZ on an empty stomach (2 h before breakfast) for 5 consecutive days, followed by 23 days without treatment, in a 28-day treatment cycle. The dose was $150 mg/m^2$ per day in the first cycle, and the dose in subsequent cycles was 100, 150, or $200 mg/m^2$ per day, based on the criteria for dose adjustment (Table 1). If adequate recovery had not occurred, the start of the next cycle was delayed until the criteria were met.

### Plasma and urine sampling

*Collection of plasma samples*

Immediately before TMZ administration (0 h) and at 15, 30, and 45 min, and 1, 1.5, 2, 3, 4, 6, 8, 12, and 24 h after administration on days 1 and 5 in the first cycle ($150 mg/m^2$) and second cycle ($200 mg/m^2$), 5 ml of venous blood was collected using a pre-chilled heparinized vacuum tube, and blood samples were cooled in an ice-water bath from immediately after sampling and centrifuged (4°C, 3000 rpm, 10 min) to separate plasma within 5 min of blood collection. For the determination of TMZ plasma concentrations, 1.0 ml of plasma sample immediately after centrifugation was placed in a polypropylene tube to which 50 µl of 8.5% phosphoric acid solution (stabilizer) had been pre-added. The acidified plasma was vortexed, and the tube was then sealed and stored frozen at −20°C or below until analysis. For determination of MTIC plasma concentrations, about 1 ml of plasma sample was dispensed immediately after centrifugation to a pre-cooled polypropylene tube. The tube was then sealed and frozen immediately on dry ice-methanol. The sample was stored frozen at −80°C or below until analysis.

**Table 1.** Dose adjustment criteria based on neutrophil count, platelet count, and onset of adverse events

| | Grade | Dose adjustment criteria based on neutrophil count and platelet count | | |
|---|---|---|---|---|
| | | 1 | 2 | 3 |
| | | Nadir neutrophil count >1500/mm$^3$ Nadir platelet count >100000/mm$^3$ | Nadir neutrophil count 1000–1500/mm$^3$ Nadir platelet count 50000–100000/mm$^3$ | Nadir neutrophil count <1000/mm$^3$ Nadir platelet count <50000/mm$^3$ |
| Dose adjustment criteria based on onset of adverse events | CTC Grade 0, 1 | Increase by 50 mg/m$^2$ per day | No change | Reduce by 50 mg/m$^2$ per day |
| | CTC Grade 2 | No change | No change | Reduce by 50 mg/m$^2$ per day |
| | CTC Grade 3, 4 | Reduce by 50 mg/m$^2$per day | Reduce by 50 mg/m$^2$ per day | Reduce by 50 mg/m$^2$ per day |

*Collection of urine samples*

Urine was collected before TMZ administration and in 0–4, 4–8, and 8- to 24-h blocks after administration on days 1 and 5 in both the first and second cycles. The total volume of urine accumulated up to each prescribed time point was collected in plastic urine collection containers to which 2 ml of 8.5% phosphoric acid solution (stabilizer) had been pre-added. These plastic containers were refrigerated throughout the urine accumulation time period. The pH of the urine in the plastic container was determined after each voiding. If the pH was 4 or more, 8.5% phosphoric acid solution was added again. Each urine sample was collected in a polypropylene tube (total, 20 ml) and the tubes were sealed and stored frozen at –20°C or below until analysis.

Assay method

TMZ and MTIC plasma concentrations were both determined by validated high-performance liquid chromatography-tandem mass spectrometry. The lower limits of quantitation of temozolomide and MTIC were 0.020 μg/ml and 5.00 ng/ml, respectively. Urinary temozolomide concentration was determined by validated high-performance liquid chromatography. The lower limit of quantitation was 1.00 μg/ml.

Pharmacokinetic analysis

The pharmacokinetic analysis of TMZ and MTIC plasma concentrations was performed by noncompartmental analysis[12] and pharmacokinetic parameters, including the maximum plasma concentration (Cmax), time-to-maximum plasma concentration (tmax), the area under the plasma concentration-time curve (AUC) up to the final observation point ($AUC_{0-t}$), AUC up to 24 h after administration ($AUC_{0-24}$), AUC up to infinite time ($AUC_{0-\infty}$), elimination half-life of terminal excretion phase ($t_{1/2}\lambda z$), apparent total body clearance (CL/F), apparent distribution volume (Vz/F), and accumulation index (R) were calculated by patient. With TMZ urinary concentrations, the amount of urinary excretion (Ae), the urinary excretion rate (Ae%), and renal clearance (CLr) were calculated for each patient.

Role of the funding source

The supporter of this study was responsible for the study design, quality assurance, and quality control systems to ensure that the study was done and data were generated, documented, analyzed, and reported in compliance with the protocol. The supporter had no role in the interpretation of the data. The corresponding author had full access to all data in the study, including those for safety, and had the final responsibility to submit the paper for publication.

## Results

Patient characteristics

Table 2 shows the major background factors of all six patients. The mean age was 43.3 years, with three patients under 40 and the remaining three between 40 and 64 years. The six patients consisted of five men and one woman. The mean body weight was 63.85 kg, and the mean body mass index was 22.92 kg/m$^2$. KPS was assessed to be 50, 60, 70, and 80 in one patient each and 90 in two patients.

According to the results of the central pathology review, one patient had anaplastic astrocytoma (AA), three had glioblastoma multiforme (GBM), one had anaplastic oligodendroglioma (AO), and one had malignant glioma. Four patients had received surgical treatment once and two had received surgical treatment twice. All patients had experienced one recurrence, and the time to recurrence was less than 6 months in one patient and 6 months or more in five patients.

Pharmacokinetics

Pharmacokinetics was examined in six patients who completed administration at 150 mg/m$^2$ per day in the first cycle and in three patients whose dose was increased to 200 mg/m$^2$ per day in the second cycle.

**Table 2.** Demographics

| Item | Classification, etc. | All subjects |
|---|---|---|
| Age (years) $n = 6$ | Mean ± standard deviation | 43.3 ± 12.4 |
| | Median value | 39.5 |
| | Minimum value–maximum value | 29–62 |
| Age classification (years) $n = 6$ | <40 | 3 (50%) |
| | ≥40 to <65 | 3 (50%) |
| | ≥65 | 0 |
| Sex $n = 6$ | Male | 5 (83%) |
| | Female | 1 (17%) |
| Body weight (kg) $n = 6$ | Mean ± standard deviation | 63.85 ± 9.14 |
| | Median value | 62.1 |
| | Minimum value–maximum value | 52.6–78.0 |
| BMI (kg/m$^2$) $n = 6$ | Mean ± standard deviation | 22.92 ± 3.71 |
| | Median value | 22.15 |
| | Minimum value–maximum value | 19.6–28.7 |
| KPS before start of administration $n = 6$ | Mean ± standard deviation | 73.3 ± 16.3 |
| | Median value | 75 |
| | Minimum value–maximum value | 50–90 |
| Central pathology judgment of lesion tissue $n = 6$ | AA | 1 (17%) |
| | Other than AA | 5 (83%) |
| Number of operations $n = 6$ | 0 | 0 |
| | 1 | 4 (67%) |
| | 2 | 2 (33%) |
| | 3 or more | 0 |
| Recurrence $n = 6$ | Once | 6 (100%) |
| | 2 Times or more | 0 |
| Duration from initial diagnosis to initial recurrence (months) $n = 6$ | <6 | 1 (17%) |
| | ≥6 | 5 (83%) |
| Steroid use $n = 6$ | No | 3 (50%) |
| | Yes | 3 (50%) |
| Most recent steroid dose[a] (mg/day) $n = 3$ | Mean ± standard deviation | 16.13 ± 0.98 |
| | Median value | 16.7 |
| | Minimum value–maximum value | 15.0–16.7 |
| Classification of most recent steroid dose[a] $n = 3$ | <10 mg/day | 0 |
| | ≥10 mg/day <20 mg/day | 3 (100%) |
| | ≥20 mg/day | 0 |

[a] Calculated as dose of prednisolone (excluding topical steroid)

*TMZ and MTIC plasma concentration-time profiles and pharmacokinetic parameters*

Table 3 shows the pharmacokinetic parameters of TMZ and MTIC plasma concentrations on days 1 and 5 of TMZ administration in the first cycle (150 mg/m$^2$ per day) and second cycle (200 mg/m$^2$ per day). Figure 1 shows the mean TMZ and MTIC concentration-time profiles on days 1 and 5 of the first and second cycles.

TMZ in the six patients in the first cycle reached tmax at about 1 h after administration, with a monophasic decrease up to 12 h after administration. TMZ plasma concentrations were below the lower limit of quantitation (0.020 μg/ml) in five of six patients after 24 h. The Cmax values on days 1 and 5 were 7.87 and 8.38 μg/ml, respectively; $AUC_{0-t}$ values were 25.7 and 25.2 μg·h/ml; $AUC_{0-24}$ values were26.5 and 25.9 μg·h/ml; and $AUC_{0-\infty}$ values were 26.1 and 25.6 μg·h/ml. The accumulation index, based on Cmax and $AUC_{0-24}$, was 1.11 and 0.986, respectively, indicating no accumulation due to repeated administration. The $t_{1/2}\lambda z$ values on days 1 and 5 of administration were 2.14 and 2.29 h, respectively; CL/F values were 2.57 and 2.56 ml/min per kg; and the Vz/F values were 0.468 and 0.492 l/kg, indicating no change due to repeated administration. These coefficients of variation for AUC, $t_{1/2}\lambda z$, CL/F, and Vz/F ranged from 9% to 35%.

As with the first cycle, TMZ in the three patients in the second cycle who received 200 mg/m$^2$ per day reached tmax at about 1 h after administration, with a monophasic decrease up to 12 h after administration. TMZ plasma concentrations were below the lower limit of quantitation in all patients after 24 h. The Cmax values on days 1 and 5 were 15.3 and 14.0 μg/ml, respectively; $AUC_{0-t}$ values were 35.1 and 36.0 μg·h/ml, $AUC_{0-24}$ values were 36.4 and 37.3 μg·h/ml; and $AUC_{0-\infty}$ values were 35.7 and 36.7 μg·h/ml. The accumulation index, based on Cmax and $AUC_{0-24}$, was 0.868 and 1.03, respectively, indicating no accumulation due to repeated administration. The $t_{1/2}\lambda z$ values on days 1 and 5 of administration were 2.03 and 2.02 h, respectively; CL/F values were 2.37 and 2.27 ml/min per kg; and Vz/F values were 0.415 and 0.395 l/kg, indicating no change due to repeated administration, and the values were nearly the same as those observed after the administration of 150 mg/m$^2$ per day. The coefficients of variation for AUC, $t_{1/2}\lambda z$, CL/F, and Vz/F ranged from 4% to 9%.

The concentration-time profile of MTIC plasma concentrations in both the first cycle (150 mg/m$^2$ per day) and the second cycle (200 mg/m$^2$ per day) was nearly parallel to that

**Table 3.** Pharmacokinetic parameters of temozolomide and MTIC plasma concentrations in cycle 1 (150 mg/m$^2$ per day) and cycle 2 (200 mg/m$^2$ per day)

| Analyte | Dose (mg/m$^2$) | Dosing day | Tmax (h) | Cmax (μg/ml) | $t_{1/2}\lambda z$ (h) | AUC (μg·h/ml) | | | CL/F (ml/min per kg) | Vz/F (l/kg) | R | |
|---|---|---|---|---|---|---|---|---|---|---|---|---|
| | | | | | | 0–t | 0–24 | 0–∞ | | | Cmax | $AUC_{0-24}$ |
| Temozolomide | 150 ($n$ = 6) | Day 1 | 1.42 (52) | 7.87 (38) | 2.14 (25) | 25.7 (15) | 26.5 (14) | 26.1 (14) | 2.57 (18) | 0.468 (23) | – | – |
| | | Day 5 | 0.958 (53) | 8.38 (36) | 2.29 (35) | 25.2 (10) | 25.9 (9) | 25.6 (10) | 2.56 (14) | 0.492 (21) | 1.11 (24) | 0.986 (8) |
| | 200 ($n$ = 3) | Day 1 | 0.583 (25) | 15.3 (5) | 2.03 (4) | 35.1 (6) | 36.4 (6) | 35.7 (6) | 2.37 (5) | 0.415 (7) | – | – |
| | | Day 5 | 0.917 (57) | 14.0 (30) | 2.02 (5) | 36.0 (4) | 37.3 (5) | 36.7 (4) | 2.27 (9) | 0.395 (5) | 0.868 (39) | 1.03 (7) |
| MTIC | 150 ($n$ = 6) | Day 1 | 1.42 (52) | 0.145 (38) | 1.98 (24) | 0.426 (15) | 0.451 (14) | 0.463 (14) | – | – | – | – |
| | | Day 5 | 1.08 (43) | 0.154 (28) | 1.83 (12) | 0.425 (12) | 0.445 (13) | 0.454 (13) | – | – | 1.14 (29) | 1.00 (16) |
| | 200 ($n$ = 3) | Day 1 | 0.750 (33) | 0.272 (15) | 1.93 (6) | 0.594 (7) | 0.622 (8) | 0.632 (8) | – | – | – | – |
| | | Day 5 | 0.917 (57) | 0.284 (33) | 1.87 (3) | 0.636 (7) | 0.665 (7) | 0.676 (7) | – | – | 1.03 (17) | 1.07 (1) |

Values are means, with coefficient of variation % in parentheses
Tmax, time of each plasma concentration; Cmax, maximun plasma concentration; $t_{1/2}\lambda z$, elimination half-life terminal excretion phase; AUC, area under the plasma concentration time curve; CL/F, apparent total body clearance; Vz/F, apparent distribution volume; R, accumulation index

of the TMZ plasma concentrations on day 1 as well as on day 5. The tmax and $t_{1/2}\lambda z$ values of MTIC plasma concentrations were 0.750 to 1.42 h and 1.83 to 1.98 h, respectively, which closely matched the tmax and $t_{1/2}\lambda z$ values of the TMZ plasma concentrations. After the administration of 150 and 200 mg/m$^2$ per day, the Cmax values were 0.145 to 0.154 and 0.272 to 0.284 μg/ml, respectively; $AUC_{0-t}$ values were 0.425 to 0.426 and 0.594 to 0.636 μg·h/ml, respectively; $AUC_{0-24}$ values were 0.445 to 0.451 and 0.622 to 0.665 μg·h/ml, respectively; and $AUC_{0-\infty}$ values were 0.454 to 0.463 and 0.632 to 0.676 μg·h/ml, respectively. Cmax and AUC exhibited a dose-dependent increase in relation to the administration of 150 mg/m$^2$ per day and 200 mg/m$^2$ per day. The ratios of MTIC to TMZ, based on Cmax and AUC, were 1.78% to 2.03% and 1.66% to 1.84%, respectively. The accumulation index, based on Cmax and $AUC_{0-24}$, was 1.03 to 1.14 and 1.00 to 1.07, indicating no accumulation due to repeated administration, as in the case of TMZ plasma concentrations. The coefficients of variation for AUC and $t_{1/2}\lambda z$ ranged from 3% to 24%.

### *TMZ urinary excretion rate*

Table 4 shows the amount of urinary excretion, excretion rate, and renal clearance by urine accumulation intervals to 24 h after the administration of TMZ on days 1 and 5 in the first cycle (150 mg/m$^2$ per day) and second cycle (200 mg/m$^2$ per day). One of the three patients in the second cycle mistakenly discarded the 0- to 4-h urine after administration on day 5, and the cumulative urinary excretion data for this patient on day 5 of the administration of 200 mg/m$^2$ per day was considered missing.

The cumulative urinary excretion rates of TMZ (up to 24 h after administration) were 7.42% and 5.93% on days 1 and 5, respectively, at 150 mg/m$^2$ per day, and 4.81% and 5.21% on days 1 and 5, respectively, at 200 mg/m$^2$ per day. The renal clearance of TMZ was 0.193 and 0.155 ml/min per kg on days 1 and 5, respectively, at 150 mg/m$^2$ per day, and 0.114 and 0.119 ml/min per kg on days 1 and 5, respectively, at 200 mg/m$^2$ per day. No change due to the difference in dose or to repeated administration was observed in the urinary excretion rate or renal clearance of TMZ. Calculation of the proportion of renal clearance to total body clearance (2.27–2.57 ml/min per kg) indicated a value of 4.81% to 7.51%.

### *Safety*

Adverse events occurred in all patients; most of these events were either mild or moderate.

The adverse events observed at an incidence of 50% or more were: constipation in 67% (four patients), nausea in 67% (four patients), increased alanine aminotransferase in 67% (four patients), increased aspartate aminotransferase in 67% (four patients), and increased blood alkaline phosphatase in 50% (three patients). These adverse events also corresponded to the adverse events for which a causal rela-

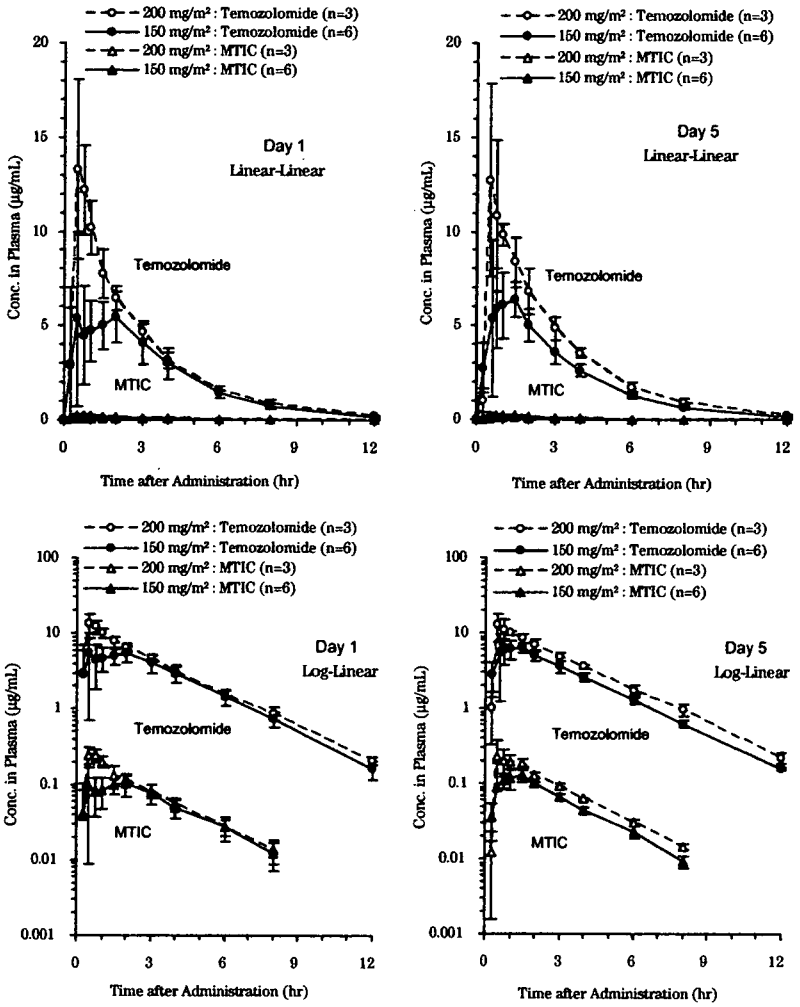


**Fig. 1.** Time-course change in mean plasma temozolomide and 5-(3-methyl)1-triazen-1-yl-imidazole-4-carboxamide (*MTIC*) concentrations on days 1 and 5 in cycle 1 (150 mg/m$^2$ per day) and cycle 2 (200 mg/m$^2$ per day)

**Table 4.** Amount of urinary temozolomide excretion (Ae), excretion rate (Ae%), and renal clearance (CLr) by urine accumulation intervals in cycle 1 (150 mg/m$^2$ per day) and cycle 2 (200 mg/m$^2$ per day)

| Parameter | Dose (mg/m$^2$) | Administration day | Time after administration (Urine accumulation interval) (h) | | | |
|---|---|---|---|---|---|---|
| | | | 0–4 | 4–8 | 8–24 | 0–24 |
| Ae (mg) | 150 | Day 1 | 11.1 (25) | 5.64 (59) | 1.49 (82) | 18.2 (22) |
| | $n = 6$ | Day 5 | 10.3 (43) | 3.37 (46) | 0.915 (55) | 14.6 (26) |
| | 200 | Day 1 | 12.8 (53) | 3.42 (62) | 0.178 (173) | 16.4 (53) |
| | $n = 3$ | Day 5 | 12.8[a] | 3.93 (32) | 1.00 (89) | 17.7[a] |
| Ae% (%) | 150 | Day 1 | 4.51 (29) | 2.32 (65) | 0.593 (80) | 7.42 (28) |
| | $n = 6$ | Day 5 | 4.20 (48) | 1.36 (47) | 0.366 (55) | 5.93 (33) |
| | 200 | Day 1 | 3.75 (57) | 1.00 (66) | 0.0524 (173) | 4.81 (57) |
| | $n = 3$ | Day 5 | 3.75[a] | 1.15 (36) | 0.300 (90) | 5.21[a] |
| CLr (ml/min per kg) | 150 | Day 1 | – | – | – | 0.193 (33) |
| | $n = 6$ | Day 5 | – | – | – | 0.155 (42) |
| | 200 | Day 1 | – | – | – | 0.114 (60) |
| | $n = 3$ | Day 5 | – | – | – | 0.119[a] |

Values are means, with coefficient of variation % in parentheses
[a] $n = 2$

tion to TMZ could not be ruled out (adverse reactions) that were observed at an incidence of 50% or more.

As myelosuppression-related adverse events, a decrease in neutrophil count (grade 2), platelet count (grade 1), and leukocyte count (grade 2) occurred in one patient each (17%). Grade 3 toxicity observed in hematology tests was a decreased lymphocyte count in one patient, and no other grade 3 or 4 toxicity was observed. Leukocyte count, platelet count, and neutrophil count were within normal ranges. No grade 3 or 4 toxicities were observed in biochemistry tests or urinalysis, except for a grade 3 increase in alanine aminotransferase in two patients.

Two adverse events resulted in death. The first was brain damage in one patient, resulting in death 23 days after the final administration in the first cycle. The second was a decreased level of consciousness in one patient who discontinued participation in the study 23 days after the final administration in the first cycle and who died about 3 months after discontinuation. The study was also discontinued in another patient 24 days after the final administration in the sixth cycle due to progression of the primary disease, and this patient died about 3.5 months after discontinuation due to aggravation of the primary disease. Three deaths occurred in this study, but the cause of death in all three patients was attributed to the primary disease.

## Discussion

We investigated the pharmacokinetics of TMZ in Japanese patients to determine whether or not the treatment regimen used in the United States and Europe could be used in Japan.

After the oral administration of 150 and 200 mg/m$^2$ per day, TMZ plasma concentration reached tmax about 1 h after administration, followed by a monophasic decrease. Although a dose-dependent increase in Cmax and AUC was observed, these values did not increase after 5 days of repeated administration (accumulation index was about 1), indicating no accumulation of this drug. The elimination of TMZ from plasma was rapid, and no change due to difference in the dose or to repeated administration was observed in CL/F or Vz/F. The coefficients of variation for AUC, $t_{1/2}\lambda z$, CL/F, and Vz/F were small, at 4% to 35%, suggesting that the interpatient difference in pharmacokinetics was small. Plasma MTIC concentrations were observed to change in parallel with TMZ plasma concentrations at both 150 and 200 mg/m$^2$ per day, and tmax and $t_{1/2}\lambda z$ values generally corresponded to those of TMZ plasma concentrations. The Cmax and AUC of MTIC plasma concentration were 1.8% to 2.0% and 1.7% to 1.8% of those of TMZ plasma concentrations. With TMZ, no accumulation was observed with repeated administration. These results suggested that the plasma MTIC concentration is dependent on the plasma TMZ concentration and that the reaction rate from MTIC to AIC is clearly more rapid than that from TMZ to MTIC. Based on the results obtained by the administration of 150 and 200 mg/m$^2$ per day, no marked change in pharmacokinetics due to the difference in dose or to repeated administration was noted. The cumulative urinary excretion rate of TMZ was 4.8% to 7.4% (up to 24 h after administration). The renal clearance of TMZ was 0.114 to 0.193 ml/min per kg, accounting for 4.8% to 7.5% of total body clearance. It is possible, however, that actual renal clearance was underestimated because of the possible effect of decomposition during the retention of urine in the bladder. The above plasma and urinary pharmacokinetic profile of TMZ in Japanese was essentially the same as that already observed in Caucasians.[8-10]

The pharmacokinetic parameters of TMZ and MTIC plasma concentrations in Japanese patients obtained in this study were compared with those obtained in pharmacokinetic studies (Schering-Plough data on file)[8,10,12] conducted

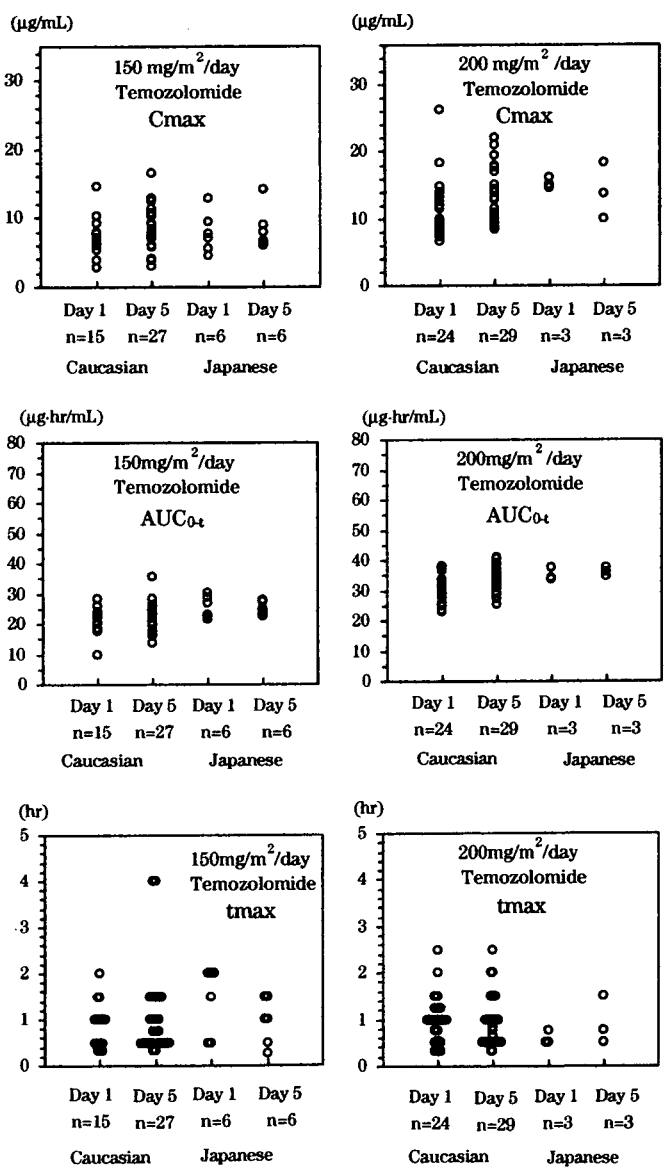


**Fig. 2.** Maximum plasma concentration (*Cmax*), area under the plasma concentration-time curve up to the final observation point ($AUC_{0\text{-}t}$), and time-to-maximum plasma concentration (*tmax*) of temozolomide: comparison between Japanese and Caucasians. Data of Caucasians are cited from Schering-Plough data on file[8,10,12]

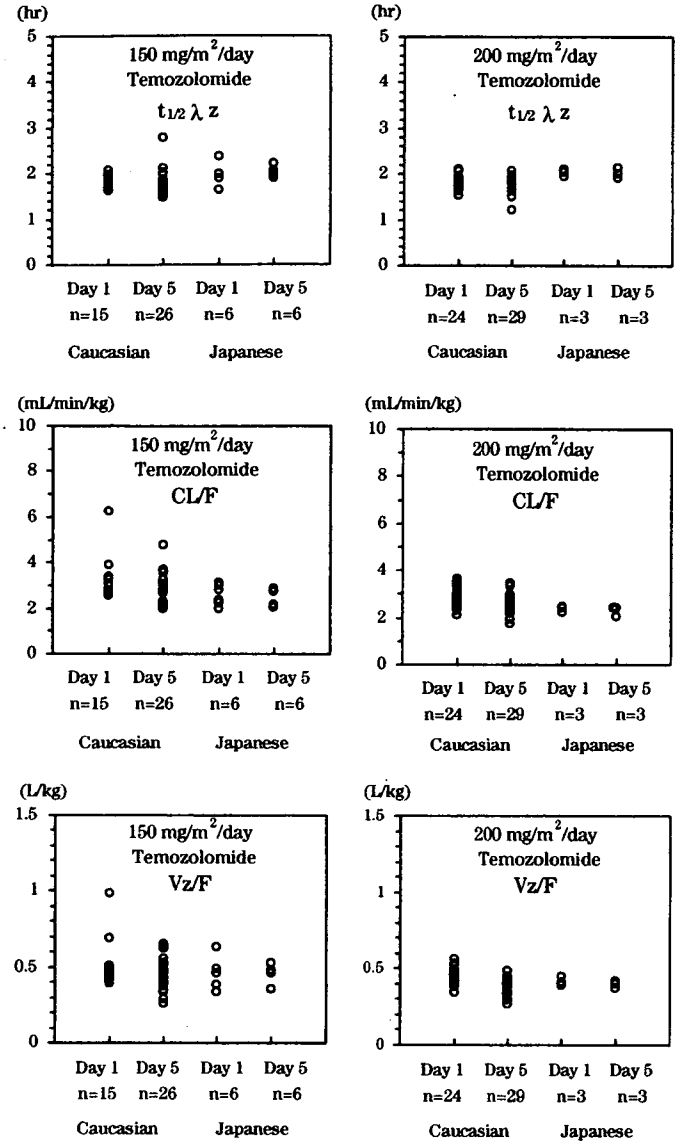


**Fig. 3.** Elimination half-life of terminal excretion phase ($t_{1/2}\lambda z$), apparent total body clearance (*CL/F*), and apparent distribution volume (*Vz/F*) of plasma temozolomide: comparison between Japanese and Caucasians. Data of Caucasians are cited from Schering-Plough data on file[8,10,12]

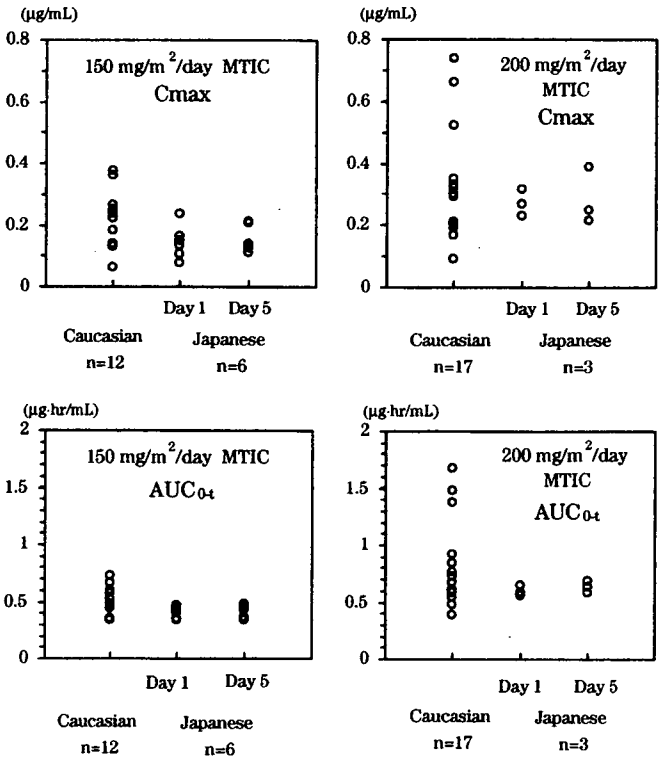


**Fig. 4.** Maximum plasma concentration (Cmax) and the area under the plasma concentration-time curve ($AUC_{0-t}$) of 5-(3-methyl)-1-triazen-1-yl-imidazole-4-carboxamide (MTIC) concentration: comparison between Japanese and Caucasians. Data of Caucasians are cited from Schering-Plough data on file[8,10,12]

in Caucasians in the United States. As shown in Figs. 2 to 5, the pharmacokinetic parameters (Cmax, tmax, $AUC_{0-t}$, $t_{1/2}\lambda z$, CL/F, and Vz/F) of plasma TMZ concentration and the pharmacokinetic parameters (Cmax, tmax, $AUC_{0-t}$, and $t_{1/2}\lambda z$) of plasma MTIC concentration obtained from Japanese patients all fell in the range of data obtained from Caucasian patients. These results confirm the assumption that there is little possibility that the pharmacokinetics of TMZ would be affected by biological factors including ethnic differences.

Adverse events occurred in all patients, but most were judged to be mild or moderate in severity. Continued administration was therefore possible with dose adjustment and delay in the start of administration of the next cycle. The incidence of nausea and constipation was high, but with prophylactic antiemetic administration during the administration period, no patient discontinued or interrupted treatment due to nausea during the 5 days of administration in each cycle. Constipation was managed with laxatives. Delay in the start of administration and dose modification due to myelosuppression was required in one of the four patients who continued to receive treatment with TMZ in the second cycle. The safe continuation of treatment was considered possible by monitoring for adverse reactions and adjusting the dose. No increase of myelosuppression with increased dose was observed.

The treatment regimen in this study was generally well tolerated in Japanese patients with relapsed gliomas.

The confirmation of the safety of TMZ in Japanese patients in this study contributes greatly to the assurance of safety in Asians, including patients in Taiwan and South Korea, where TMZ is already being used. The possibility is very high that the treatment regimen in the United States and Europe is applicable to all ethnic groups.

## Conflict of interest

All authors declare no conflict of interest.

**Acknowledgments** This study was supported by Schering-Plough K.K. We are indebted to the patients and their families for agreeing to par-

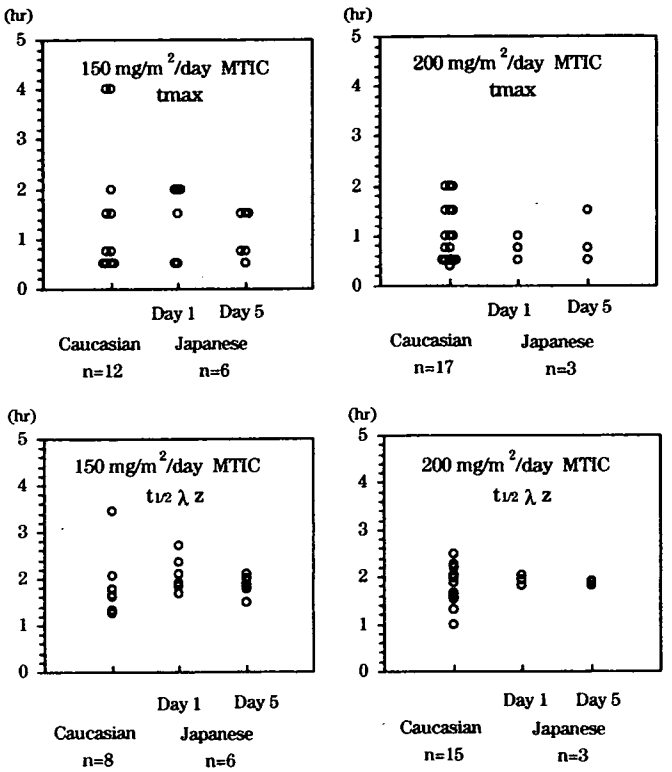


**Fig. 5.** Values for time of each plasma concentration (tmax) and terminal excretion phase ($t_{1/2}\lambda z$) of plasma 5-(3-methyl)-1-triazen-1-yl-imidazole-4-carboxamide (MTIC) concentration: comparison between Japanese and Caucasians. Data of Caucasians are cited from Schering-Plough data on file[8,10,12]

ticipate in this study, and to the study nurse and data managers for their collaboration.

## References

1. Slack JA, Goddard C, Stevens MFG, et al. (1986) The analysis and murine pharmacokinetics of a new antitumor agent: CCRG 81045. J Pharm Pharmacol 38:63
2. Wheelhouse RT, Stevens MFG (1993) Decomposition of the antitumor drug temozolomide in deuteruated phosphate buffer: methyl group transfer is accompanied by deuterium exchange. J Chem Soc Chem Commun 15:1177–1178
3. Denny BJ, Wheelhouse RT, Stevens MFG, et al. (1994) NMR and molecular modeling investigation of the mechanism of activation of the antitumor drug temozolomide and its interaction with DNA. Biochemistry 33:9045–9051
4. Stevens MFG, Hickman JA, Langdon SP, et al. (1987) Antitumor activity and pharmacokinetics in mice of 8-carbamoyl-3-methyl-imidazo [5,1-d]-1,2,3,5-tetrazin-4(3H)-one (CCRG 81045: M&B 39831), a novel drug with potential as an alternative to dacarbazine. Cancer Res 47:5846–5852
5. Newlands ES, Stevenst MFG, Wedge SR, et al. (1997) Temozolomide: a review of its discovery, chemical properties, pre-clinical development and clinical trials. Cancer Treat Rev 23:35–61
6. Ostermann S, Csajka C, Buclin T, et al. (2004) Plasma and cerebrospinal fluid population pharmacokinetics of temozolomide in malignant glioma patients. Clin Cancer Res 10:3728–3736
7. Newlands ES, Blackledge GRP, Slack JA, et al. (1992) Phase I trial of temozolomide (CCRG 81045: M&B 39831: NSC 362856). Br J Cancer 65:287–291
8. Brada M, Judson I, Beale P, et al. (1999) Phase I dose-escalation and pharmacokinetic study of temozolomide (SCH 52365) for refractory or relapsing malignancies. Br J Cancer 81:1022–1030
9. Rudek MA, Donehouwer RC, Statkevich P, et al. (2004) Temozolomide in patients with advanced cancer: phase I and pharmacokinetic study. Pharmacotherapy 24:16–25
10. Beale P, Judson I, Moore S, et al. (1999) Effect of gastric pH on the relative oral bioavailability and pharmacokinetics of temozolomide. Cancer Chemother Pharmacol 44:389–394
11. Kleihues P, Louis DN, Scheithauer BW, et al. (2002) The WHO classification of tumors of the nervous system. J Neuropathol Exp Neurol 61:215–225; discussion 226–229
12. Hammond LA, Eckardt JR, Baker SD, et al. (1999) Phase I and pharmacokinetic study of temozolomide on a daily-for-5-days schedule in patients with advanced solid malignancies. J Clin Oncol 17:2604–2613

# 膠芽腫(脳幹，延髄，上位頸髄)

西川　亮

## はじめに

脳幹部神経膠腫の約1/4は組織学的にWHO grade IないしIIと考えられ，比較的長い臨床経過をたどることが知られている(表1)[1,2]．一方最も頻度の高いdiffuse intrinsic typeのびまん性脳幹部神経膠腫は，その占拠および進展部位から手術は行われないことが多いが，組織学的にはWHO grade IIIないしIVである場合が多いとされている．臨床的にも極めて悪性の経過をたどり，標準的な生存期間はわずか9ヵ月である．

本特集の主題である頭蓋頸椎移行部の神経膠腫は，狭義には，長い臨床経過をたどり手術の対象となることが多く，ほとんどの場合組織型はlow-grade gliomaである腫瘍群を指す[2,3]．しかし本稿に与えられたテーマは膠芽腫，すなわち悪性度の高い腫瘍群であるので，この悪性度の低い，いわゆるcervicomedullary gliomaの解説は別稿に譲り，diffuse intrinsic typeのびまん性脳幹部神経膠腫を中心に解説してみたい．

にしかわ りょう　埼玉医科大学教授/国際医療センター包括的がんセンター脳脊髄腫瘍科

## びまん性脳幹部神経膠腫

### 1．症候，診断

5〜10歳に好発する．病状の進行は急速で発症から発見までの期間の中央値は1ヵ月である．脳神経症状，long tract sign，小脳失調を三主徴とする．脳幹部の中では橋に発生することが圧倒的に多いため，脳神経症状としては顔面神経麻痺と外転神経麻痺が高頻度であり初発症状になり

脳幹部神経膠腫のMRI画像
左）ガドリニウム造影T1強調画像，右）T2強調画像．9歳女性．左外転神経麻痺，左末梢性顔面神経麻痺，右片麻痺，右優位の小脳性失調を認めた．

表1　脳幹部神経膠腫の分類

| タイプ | 頻　度 | 年　齢 | 臨床症状 | 代表的な組織型 | 治　療 | 生存期間中央値 |
|---|---|---|---|---|---|---|
| Focal tectal | 5% | 年長児〜成人 | 水頭症，頭蓋内圧亢進 | Diffuse astrocytoma | シャント，経過観察 | 7年以上 |
| Dorsal exophytic | 10-15% | 3歳 | 水頭症，頭蓋内圧亢進 | Pilocytic astrocytoma | 手術＋放射線照射/化学療法 | 5年以上 |
| Cervicomedullary | 5% | All | 下位脳神経症状，片麻痺 | Diffuse astrocytoma | 手術＋放射線照射/化学療法 | 5年以上 |
| Diffuse intrinsic | 80% | 7歳 | 早い臨床経過．多発両側性の脳神経症状，片麻痺，失調 | Astrocytic tumors (WHO grade III/IV) | 放射線照射/化学療法 | 1年以下 |

(Freemanら[1]，西川[2]より改変)



0289-0585/07/¥500/論文/JCLS